cesses, might interact with synucleinopathy as a pathologic network that contributes to PD development and progression, even at premotor stages. In addition to experiments showing that both tau and Aβ might directly interact with α-synuclein, facilitating its aggregation,[17,18] this argument is further supported by recent independent genome-wide association studies indicating that the *SNCA* and *MAPT* genes/regions (encoding α-synuclein and tau, respectively) are consistently associated with an increased risk of developing PD.[19,20]

Our results, if applicable to sporadic PD, also suggest that $A\beta_{42}$ and tau could potentially be used as biomarkers for early PD diagnosis. However, since they are not particularly strong predictors of the disease condition, it is likely that a combination of $A\beta_{42}$ and tau with other markers will be necessary for effective preclinical diagnosis or monitoring disease progression. A major limitation in focusing on *LRRK2* mutation carriers is that this approach is logistically difficult in that it requires recruitment from a very limited pool of subjects, lengthy and potentially uncomfortable procedures (PET imaging and lumbar puncture), and in many instances, international travel. Thus, we were only able to study a modest number of participants, and because this was an exploratory study we did not perform statistical correction for multiple comparisons. Therefore, the data need to be interpreted with caution and the results should be replicated, ideally using a longitudinal design with serial PET scans and CSF measurements.

AUTHOR CONTRIBUTIONS

J.Z. conceived and supervised the project, and drafted the manuscript with M.S., J.O.A., T.S., and K.K.J., J.O.A., K.K.J., Z.K.W., R.J.U., K.H., T.Y., C.P.Z., H.M.K., and J.B.L. were responsible for patient characterization and sample collection. M.S. assisted in experimental design and execution, as well as in data interpretation and statistical analyses. V.S. and A.J.S. were responsible for PET analysis. C.G. worked on CSF sample handling and Luminex assays. J.A. worked on data management and statistical analyses. K.L.E. and K.W.S. were involved in statistical analyses. All authors critically reviewed the manuscript.

ACKNOWLEDGMENT

The authors thank Sydney Thomas for study coordination; Joshua Bradner for data analysis; Dr. Amy Furay for critical review of the manuscript and copyediting; Jennifer Lash for assistance making arrangements for some research subjects involved in this study for their travel to Seattle, WA, and Vancouver, BC; and the patients for their participation and sample donations.

STUDY FUNDING

Supported by NIH (AG025327, AG033398, P30ES007033-6364, ES004696-5897, ES012703, ES016873, NS057567, NS060252 to J.Z., P50NS062684 to C.P.Z., J.B.L., and J.Z., NS065070 to C.P.Z., NS057567 and P50NS072187 to Z.K.W. and R.J.U.), Department of Veterans Affairs (to J.B.L. and H.M.K., and 1101BX000531 to C.P.Z.), Canadian Institutes of Health Research (to A.J.S.), Michael Smith Foundation for Health Research (to A.J.S.), Pacific Alzheimer Research Foundation (to A.J.S.), Canada Research Chairs program (to A.J.S.), TRIUMF (to A.J.S.), Mayo Clinic Florida Research Committee CR program (to Z.K.W. and R.J.U.), the gift from Carl Edward Bolch, Jr. and Susan Bass Bolch (to Z.K.W. and R.J.U.), and Grants-in-Aid from the Research Committee of CNS Degenerative Diseases, the Ministry of Health, Labour and Welfare of Japan (to K.H. and T.Y.).

DISCLOSURE

Dr. Aasly serves on the editorial boards of *Parkinsonism and Related Disorders*, *Parkinson's Disease*, and the *Journal of the Norwegian Medical Association*; and his institution receives annual royalties from Lundbeck Inc. from the licensing of the technology related to PARK8/LRRK2. Dr. Shi reports no disclosures. Dr. Sossi has received research support from Pacific Alzheimer Research Foundation. Dr. Stewart and Dr. Johansen report no disclosures. Dr. Wszolek serves as Co-Editor-in-Chief of *Parkinsonism and Related Disorders*, Regional Editor of the *European Journal of Neurology*, and on the editorial boards of *Neurologia i Neurochirurgia Polska*, *Advances in Rehabilitation*, the *Medical Journal of the Rzeszow University*, and *Clinical and Experimental Medical Letters*; holds and has contractual rights for receipt of future royalty payments from patents re: A novel polynucleotide involved in heritable Parkinson's disease; receives royalties from publishing *Parkinsonism and Related Disorders* (Elsevier, 2007, 2008, 2009) and the *European Journal of Neurology* (Wiley-Blackwell, 2007, 2008, 2009); and receives research support from Allergan, Inc., the NIH/NINDS, Mayo Clinic Florida Research Committee CR program, the Pacific Alzheimer Research Foundation (Canada), the CIHR, the Mayo Clinic Florida Research Committee CR program, and a gift from Carl Edward Bolch, Jr., and Susan Bass Bolch. Dr. Uitti serves as an Associate Editor of *Neurology*®; has received research support from Advanced Neuromodulations Systems and from the NIH; and his institution receives annual royalties from Lundbeck Inc. from the licensing of the technology related to PARK8/LRRK2. Dr. Hasegawa and Dr. Yokoyama report no disclosures. Dr. Zabetian has received research support from NIH (NINDS/NIA), the US Department of Veterans Affairs, the Parkinson's Disease Foundation, and the American Parkinson Disease Association. Dr. Kim reports no disclosures. Dr. Leverenz has served as a consultant for Bayer Schering Pharma, Novartis, and Teva Pharmaceutical Industries Ltd.; has received speaker honoraria from Novartis; and receives research support from the NIH/NIND, the Michael J. Fox Foundation, the Washington Chapter American Parkinson's Disease Association/Northwest Collaborative Care, and the US Department of Veterans Affairs. Dr. Ginghina and J. Armaly report no disclosures. Dr. Edwards has received research support from the NIH and the Centers for Disease Control. K.W. Snapinn has received research support from the NIH, the US Department of Veterans Affairs, and the Centers for Disease Control. Dr. Stoessl serves on a scientific advisory board for Biovail Corporation/Medgenesis; has received funding for travel and speaker honoraria from Novartis, Teva Pharmaceutical Industries Ltd., Allergan, Inc., and Abbott; serves on the editorial boards of *Annals of Neurology*, *Lancet Neurology*, and *Parkinsonism & Related Disorders*; and receives research support from CIHR, the Michael Smith Foundation for Health Research, the Michael J. Fox Foundation, and the Pacific Alzheimer Research Foundation. Dr. Zhang serves on the editorial boards of *Neurological Disease*, *Neurochemical Research*, the *Journal of Alzheimer's Disease*, and *Proteomics*; and has received research support from the NIH.

Received June 14, 2011. Accepted in final form September 7, 2011.

REFERENCES

1. Shi M, Zhang J. Cerebrospinal fluid α-synuclein, tau and amyloid β in Parkinson's disease. Lancet Neurol 2011;10:681.
2. Shi M, Bradner J, Hancock AM, et al. Cerebrospinal fluid biomarkers for Parkinson disease diagnosis and progression. Ann Neurol 2011;69:570–580.
3. Mollenhauer B, Locascio JJ, Schulz-Schaeffer W, Sixel-Döring F, Trenkwalder C, Schlossmacher MG. α-Synuclein and tau concentrations in cerebrospinal fluid of patients presenting with parkinsonism: a cohort study. Lancet Neurol 2011;10:230–240.

4. Abdo WF, Bloem BR, Van Geel WJ, Esselink RA, Verbeek MM. CSF neurofilament light chain and tau differentiate multiple system atrophy from Parkinson's disease. Neurobiol Aging 2007;28:742–747.
5. Alves G, Bronnick K, Aarsland D, et al. CSF amyloid-beta and tau proteins, and cognitive performance, in early and untreated Parkinson's disease: the Norwegian ParkWest study. J Neurol Neurosurg Psychiatry 2010;81:1080–1086.
6. Montine TJ, Shi M, Quinn JF, et al. CSF Abeta42 and tau in Parkinson's disease with cognitive impairment. Mov Disord 2010;25:2682–2685.
7. Wu Y, Le W, Jankovic J. Preclinical biomarkers of Parkinson disease. Arch Neurol 2011;68:22–30.
8. Kumari U, Tan EK. LRRK2 in Parkinson's disease: genetic and clinical studies from patients. FEBS J 2009;276:6455–6463.
9. Haugarvoll K, Wszolek ZK. Clinical features of LRRK2 parkinsonism. Parkinsonism Relat Disord 2009;15(suppl 3):S205–208.
10. Adams JR, van Netten H, Schulzer M, et al. PET in LRRK2 mutations: comparison to sporadic Parkinson's disease and evidence for presymptomatic compensation. Brain 2005;128:2777–2785.
11. Nandhagopal R, Mak E, Schulzer M, et al. Progression of dopaminergic dysfunction in a LRRK2 kindred: a multitracer PET study. Neurology 2008;71:1790–1795.
12. Compta Y, Marti MJ, Ibarretxe-Bilbao N, et al. Cerebrospinal tau, phospho-tau, and beta-amyloid and neuropsychological functions in Parkinson's disease. Mov Disord 2009;24:2203–2210.
13. Siderowf A, Xie SX, Hurtig H, et al. CSF amyloid β 1–42 predicts cognitive decline in Parkinson disease. Neurology 2010;75:1055–1061.
14. Litvan I, Halliday G, Hallett M, et al. The etiopathogenesis of Parkinson disease and suggestions for future research: part I. J Neuropathol Exp Neurol 2007;66:251–257.
15. Wills J, Jones J, Haggerty T, Duka V, Joyce JN, Sidhu A. Elevated tauopathy and alpha-synuclein pathology in postmortem Parkinson's disease brains with and without dementia. Exp Neurol 2010;225:210–218.
16. Haass C, Selkoe DJ. Soluble protein oligomers in neurodegeneration: lessons from the Alzheimer's amyloid beta-peptide. Nat Rev Mol Cell Biol 2007;8:101–112.
17. Clinton LK, Blurton-Jones M, Myczek K, Trojanowski JQ, LaFerla FM. Synergistic Interactions between Abeta, tau, and alpha-synuclein: acceleration of neuropathology and cognitive decline. J Neurosci 2010;30:7281–7289.
18. Tsigelny IF, Crews L, Desplats P, et al. Mechanisms of hybrid oligomer formation in the pathogenesis of combined Alzheimer's and Parkinson's diseases. PLoS ONE 2008;3:e3135.
19. Pankratz N, Wilk JB, Latourelle JC, et al. Genomewide association study for susceptibility genes contributing to familial Parkinson disease. Hum Genet 2009;124:593–605.
20. Simon-Sanchez J, Schulte C, Bras JM, et al. Genome-wide association study reveals genetic risk underlying Parkinson's disease. Nat Genet 2009;41:1308–1312.

The Nitric Oxide-Cyclic GMP Pathway Regulates FoxO and Alters Dopaminergic Neuron Survival in *Drosophila*

Tomoko Kanao[1], Tomoyo Sawada[4,5], Shireen-Anne Davies[6], Hiroshi Ichinose[7], Kazuko Hasegawa[8], Ryosuke Takahashi[4,5], Nobutaka Hattori[2,5], Yuzuru Imai[3]*

1 Research Institute for Diseases of Old Age, Juntendo University Graduate School of Medicine, Tokyo, Japan, **2** Department of Neurology, Juntendo University Graduate School of Medicine, Tokyo, Japan, **3** Department of Neuroscience for Neurodegenerative Disorders, Juntendo University Graduate School of Medicine, Tokyo, Japan, **4** Department of Neurology, Kyoto University Graduate School of Medicine, Kyoto, Japan, **5** CREST (Core Research for Evolutionary Science and Technology), JST, Saitama, Japan, **6** Institute of Molecular, Cell and Systems Biology, College of Medical, Veterinary and Life Sciences, University of Glasgow, Glasgow, Scotland, United Kingdom, **7** Department of Life Science, Graduate School of Bioscience and Biotechnology, Tokyo Institute of Technology, Yokohama, Japan, **8** Department of Neurology, National Hospital Organization, Sagamihara National Hospital, Sagamihara, Japan

Abstract

Activation of the forkhead box transcription factor FoxO is suggested to be involved in dopaminergic (DA) neurodegeneration in a *Drosophila* model of Parkinson's disease (PD), in which a PD gene product LRRK2 activates FoxO through phosphorylation. In the current study that combines *Drosophila* genetics and biochemical analysis, we show that cyclic guanosine monophosphate (cGMP)-dependent kinase II (cGKII) also phosphorylates FoxO at the same residue as LRRK2, and *Drosophila* orthologues of cGKII and LRRK2, DG2/For and dLRRK, respectively, enhance the neurotoxic activity of FoxO in an additive manner. Biochemical assays using mammalian cGKII and FoxO1 reveal that cGKII enhances the transcriptional activity of FoxO1 through phosphorylation of the FoxO1 S319 site in the same manner as LRRK2. A *Drosophila* FoxO mutant resistant to phosphorylation by DG2 and dLRRK (dFoxO S259A corresponding to human FoxO1 S319A) suppressed the neurotoxicity and improved motor dysfunction caused by co-expression of FoxO and DG2. Nitric oxide synthase (NOS) and soluble guanylyl cyclase (sGC) also increased FoxO's activity, whereas the administration of a NOS inhibitor L-NAME suppressed the loss of DA neurons in aged flies co-expressing FoxO and DG2. These results strongly suggest that the NO-FoxO axis contributes to DA neurodegeneration in *LRRK2*-linked PD.

Citation: Kanao T, Sawada T, Davies S-A, Ichinose H, Hasegawa K, et al. (2012) The Nitric Oxide-Cyclic GMP Pathway Regulates FoxO and Alters Dopaminergic Neuron Survival in *Drosophila*. PLoS ONE 7(2): e30958. doi:10.1371/journal.pone.0030958

Editor: Philipp J. Kahle, Hertie Institute for Clinical Brain Research and German Center for Neurodegenerative Diseases, Germany

Received September 18, 2011; **Accepted** December 28, 2011; **Published** February 29, 2012

Funding: This study was supported by funding from the Inamori Foundation, the Uehara Memorial Foundation, Dainippon Sumitomo Pharma, and the Program for Young Researchers from Special Coordination Funds for Promoting Science and Technology commissioned by MEXT in Japan. The funders had no role in study design, data collection and analysis, decision to publish, or preparation of the manuscript.

Competing Interests: The authors have read the journal's policy and have the following conflicts: this work was partly supported by Dainippon Sumitomo Pharma. This does not alter the authors' adherence to all the PLoS ONE policies on sharing data and materials.

* E-mail: yzimai@juntendo.ac.jp

Introduction

PD, one of the most common movement disorders, is characterized by age-dependent impairments of several nervous systems including the midbrain DA system. The degeneration of DA neurons in the substantia nigra produces the prominent motor symptoms of PD. Postmortem inspections and studies with neurotoxin-based PD models suggest a multifactorial etiology involving inflammation, mitochondrial dysfunction, iron accumulation and oxidative stress. NO, a free gaseous signaling molecule, has also been implicated in PD [1,2]. The signaling function of NO is dependent on the dynamic regulation of its synthase, NOS. There are three types of NOS, neuronal NOS (nNOS), endothelial NOS (eNOS) and inducible NOS (iNOS), in humans whereas the *Drosophila* genome has only a single orthologue, dNOS. High levels of nNOS and iNOS have been reported in the substantia nigra of PD patients [3,4] and animal models of PD [5,6]. Overproduction of NO is suggested to cause DNA damage, protein modifications and cell toxicity mainly mediated by the reactive species peroxynitrite, which may be generated with dopamine metabolism in DA neurons. In the etiology of PD, overproduction of NO could be caused either by upregulation of iNOS in activated glia cells [3,5] or by an increase in intracellular calcium, for example, after glutamate excitotoxicity [7].

The discovery of genes linked to rare familial forms of PD has provided vital clues to understanding the cellular and molecular pathogenesis of the disease. Missense mutations in the *Leucine-rich repeat kinase 2 (LRRK2)/Dardarin* gene cause autosomal dominant late onset familial PD as well as sporadic PD [8,9,10]. The clinical symptoms and pathology caused by *LRRK2* mutations closely resemble those of the sporadic form of PD, suggesting that the LRRK2 pathogenic pathway may underlie the general PD etiology. The *LRRK2* gene encodes a large protein with multiple domains including a GTPase domain and a kinase domain [8,9]. Several amino acid substitutions are identified as pathogenic mutations linked to PD [11]. Mutations in the kinase domain of human LRRK2 such as G2019S and I2020T have been reported to produce enhanced kinase activity *in vitro*, suggesting that gain-of-function mutations of LRRK2 cause neurodegeneration [12,13,14]. However, how these mutations present in the LRRK2 gene lead to the progressive loss of DA neurons and other associated pathologies is still unknown.

Because various key signaling pathways are conserved between humans and *Drosophila*, genetic and functional studies using *Drosophila* models for familial PD have revealed crucial signal transductions that affect the pathogenesis of PD [15]. We have previously reported that a *Drosophila* LRRK2 orthologue, dLRRK phosphorylates *Drosophila* FoxO (dFoxO) at Ser259, which stimulates the expression of a pro-apoptotic dFoxO target, *hid*, and leads to neurodegeneration in *Drosophila* [16]. The event was further enhanced by transgenic expression of pathogenic dLRRK proteins such as dLRRK I1915T (corresponding to I2020T in humans). However, a kinase-dead form of dLRRK (dLRRK 3KD) did not completely suppress a synergic effect caused by the co-expression of dFoxO with dLRRK, suggesting that some other factor(s) modulates this pathway. Here, we report that cGKII also phosphorylates FoxO and activates FoxO-transcriptional activity in the same manner as LRRK2/dLRRK by using biochemical studies of mammalian cGKII and FoxO1. Moreover, by using *Drosophila* models, our data suggest that NO signaling and its downstream effector cGKII/DG2 contribute to DA neurodegeneration.

Results

cGK genetically interacts with FoxO and activates FoxO activity

We previously reported a genetic interaction between FoxO and LRRK2/dLRRK in *Drosophila* [16]. To identify components of the LRRK2-FoxO signaling pathway, we screened for modifiers (Fig. 1 and Fig. S1A). Kinases reported to affect the activity of FoxO were expressed with dFoxO in the *Drosophila* eye. As reported, transgenic expression of AKT suppressed FoxO-mediated developmental defects in the eye. The expression of MST/Hippo resulted in extensive degeneration, which did not appear to be dependent on FoxO (Fig. 1). Expression of one of the *Drosophila* cGMP-dependent kinases (cGKs), DG2, leads to strong optic degeneration in conjunction with dFoxO (Fig. 1 and Fig. S2A), while the other kinases had little effect on the developmental defects caused by FoxO (Fig. 1). Removal of one copy of the *dg2* gene improved the defects, suggesting that endogenous DG2 activity contribute to the dFoxO-mediated neurodegeneration (Fig. 2H compared with B).

Next we examined whether DG2 is an upstream kinase of dLRRK, or whether DG2 acts independently of dLRRK by means of a combination of genetic interaction tests, reporter assays for FoxO and *in vitro* kinase assay. Co-expression of dLRRK harboring a PD-related mutant I1915T together with DG2 dramatically enhanced the toxicity of dFoxO (Fig. 2D compared with C). However, expression of dLRRK 3KD or removal of the dLRRK gene did not suppress the eye phenotype caused by dFoxO-DG2 at all (Fig. 2E and J compared with C). Co-expression of DG2 and dLRRK I1915T produced a normal eye, suggesting that the phenotype is dependent on the level of dFoxO protein (Fig. 2I compared with D).

Co-expression of dFoxO with DG2, but not GFP or DG1, in *Drosophila* eyes caused appearance of a slower migrated dFoxO protein in western blot analysis (Fig. 3A), which indicates phosphorylation of dFoxO [16]. Consistent with the result, knockdown of DG2 decreased a phosphorylated form of endogenous dFoxO in *Drosophila* brain tissue (Fig. 3B). In *Drosophila* S2 cells, transient expression of DG2 together with 8-bromoguanosine-3′, 5′-cyclic monophosphate (8-Br-cGMP), a membrane permeable analogue for cGMP, also stimulates phosphorylation of endogenous dFoxO (Fig. 3C, lane 3).

Two groups of cGKs, the soluble type I (cGKI α and β) and the membrane-bound type II (cGKII), have been reported in vertebrates. In *Drosophila*, there are two genes encoding cGK, namely *dg1* and *dg2* [17]. As reported [18], the gene products DG1 and DG2 are located in the cytoplasm and at the cytoplasmic membrane, respectively (Fig. 3E and F). Interestingly, expression of DG1 had little effect on the degeneration of the eye mediated by dFoxO, suggesting that DG1 and DG2 have different roles *in vivo* (Fig. S1B, S2B and S2C). Although predictions of amino acid sequence indicate that DG2 is more similar as a cGKI α/β homologue [19], their subcellular distribution suggests that DG2 is functionally more similar to cGKII (Fig. 3G–J) [18,20,21]. Consistent with the idea, transgenic expression of human cGKII exacerbated eye degeneration by dFoxO (Fig. 2G compared with B) whereas expression of cGKII alone did not affect the eye development (Fig. 2F). Interestingly, cGKII appeared to recruit FoxO1 to the cytoplasmic membrane of human cultured cells (Fig. 3K–M) while there was no evidence that cGKI associates with cGKII *in vivo* (Fig. S3). In addition, we observed that cGKII is

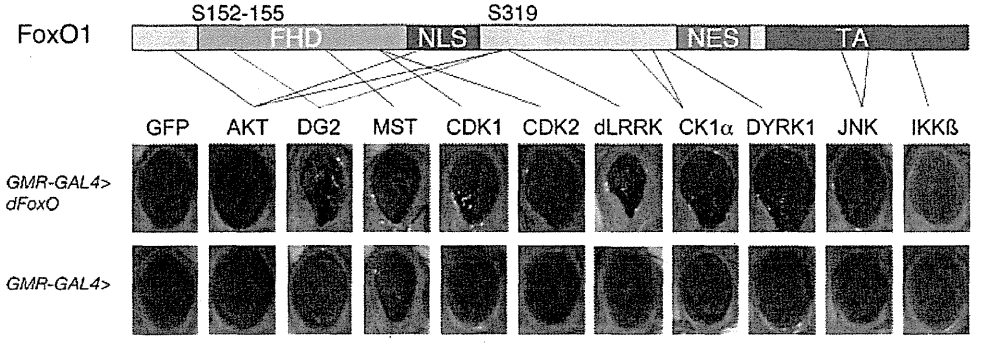

Figure 1. Screening of kinases that affect the eye phenotypes caused by dFoxO. *Drosophila* orthologues of reported FoxO kinases were expressed with (upper row) or without (lower) dFoxO in *Drosophila* eyes using the *GMR-GAL4* driver. GFP served as a control. The *Drosophila* DG2 is presumably functionally equivalent to the vertebrate cGKII. Reported phosphorylation sites and newly identified sites that are phosphorylated by cGKII (S152–155 and S319) in human FoxO1 are indicated by black and red lines, respectively. FHD, forkhead domain; NLS, nuclear localization signal; NES, nuclear export signal; TA, transactivation domain. Overexpressing lines used for crosses are: *UAS-GFP* (GFP), *UAS-AKT1* (AKT), *UAS-DG2* (DG2), *UAS-hippo* (MST), *UAS-CDK1-Myc* (CDK1), *UAS-CDK2-Myc* (CDK2), *UAS-dLRRK* (dLRRK), $Ckl\alpha^{EP1555}$ (CK1α), $mnb^{EY14320}$ (DYRK1), *UAS-bsk* (JNK), *UAS-dIKKß* (IKKβ).

doi:10.1371/journal.pone.0030958.g001

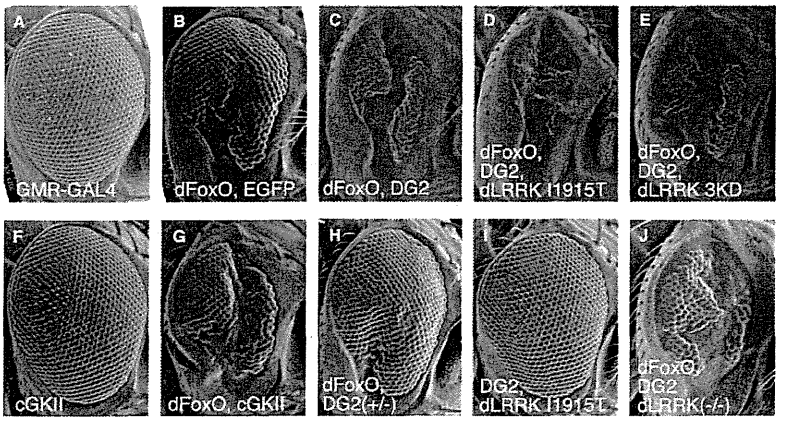

Figure 2. DG2 as well as dLRRK additively enhances FoxO-mediated developmental defects in the *Drosophila* eye. (**A–J**) SEM images of the eye of flies expressing the indicated genes. The genotypes are: *GMR-Gal4* (**A**), *GMR-Gal4/UAS-EGFP* (**B**), *UAS-DG2; GMR-Gal4, UAS-dFoxO* (**C**), *UAS-DG2; GMR-Gal4, UAS-dFoxO; UAS-dLRRK I1915T* (**D**), *UAS-DG2; GMR-Gal4, UAS-dFoxO; UAS-dLRRK 3KD* (**E**), *GMR-Gal4; UAS-cGKII* (**F**), *GMR-Gal4, UAS-dFoxO; UAS-cGKII* (**G**), *GMR-Gal4, UAS-dFoxO/DG2^{k04703}* (**H**), *UAS-DG2; GMR-Gal4; UAS-dLRRK I1915T* (**I**), *UAS-DG2; GMR-Gal4, UAS-dFoxO; e03680/e03680* (**J**).
doi:10.1371/journal.pone.0030958.g002

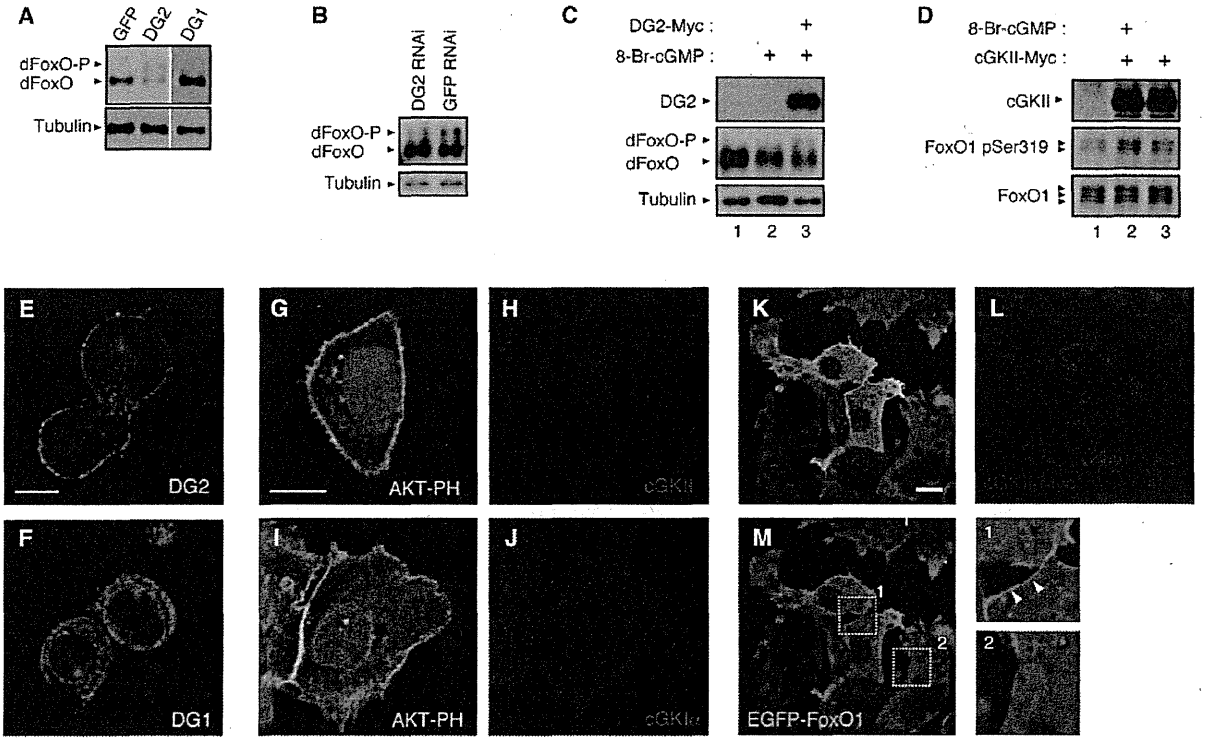

Figure 3. DG2 modulates FoxO *in vivo*. (**A**) dFoxO and the indicated transgenes were expressed in the *Drosophila* eyes using the *GMR-GAL4* driver. Extracts from brain tissues were subjected to western blot analysis. dFoxO-P; a phosphorylated form of dFoxO. (**B**) DG2 RNAi or GFP RNAi constructs were expressed in the *Drosophila* brain using the *elav-GAL4* driver. Western blot analysis for endogenous dFoxO was carried out as in (**A**). (**C**) *Drosophila* S2 cells were transfected with or without C-terminally Myc-tagged DG2 (DG2-Myc). Thirty-six hrs post transfection, cells were treated with or without 10 μM 8-Br-cGMP for 30 min. Cell lysate were then subjected to western blot analysis. (**D**) Human 293T cells were transfected with or without cGKII-Myc, and were treated with 8-Br-cGMP as in (**C**). Phosphorylation of the S319 site in endogenous FoxO1 was detected with phospho-specific antibody. (**E, F**) S2 cells expressing DG2-Myc (**E**) or DG1-Myc (**F**) were visualized with anti-Myc antibody (green), by counterstaining with DAPI (blue color). (**G–J**) HeLa cells expressing AKT-PH-GFP (green) along with cGKII-Myc (**G, H**) or cGKI-Myc (**I, J**) were visualized with anti-Myc antibody (red), by counterstaining with DAPI (blue color). AKT-PH-GFP was used for a marker protein of the plasma membrane [62]. (**K–M**) Flp-In T-REx-293 cells harboring EGFP-FoxO1 gene were transiently transfected with cGKII-Myc, and EGFP-FoxO1 was induced with doxycycline. Enlarged views of the plasma membrane regions in cGKII-positive (Box1) and negative (Box2) cells are also shown in (**M**). Accumulation of FoxO1 along with cGKII in the plasma membrane is indicated by arrowheads. Scale bars = 5 μm for (**E, F**), 25 μm for (**G–J**) and 10 μm for (**K–M**).
doi:10.1371/journal.pone.0030958.g003

abundantly expressed in DA neurons in the substantia nigra of mice (Fig. S4). We then focused on mammalian cGKII as a cGK that might be associated with the pathology of PD. Reporter assays for FoxO transcriptional activity revealed that cGKII stimulated FoxO activity in cultured mammalian cells and that co-expression of hLRRK2 with cGKII caused a 3-fold increase in FoxO activity (Fig. 4A). A kinase-dead form of hLRRK2 (hLRRK2 3KD) did not suppress the activation of FoxO by cGKII to the control level. Similarly, a kinase-dead form of cGKII (cGKII KD) failed to suppress FoxO's activation by LRRK2 (Fig. 4B). The results of the genetic interaction tests and the reporter assays suggested that cGKII and LRRK2 have additive effects on the regulation of FoxO activity.

cGK directly phosphorylates FoxO in vitro

Previously, we have demonstrated that LRRK2 phosphorylates, and enhances the neurotoxic activity of, FoxO. Using *in vitro* kinase assays, we tested whether cGKII stimulates the kinase activity of LRRK2 through phosphorylation, or whether cGKII directly activates FoxO as shown in a study on LRRK2 [16]. We transfected HEK293 cells with a FLAG-tagged cGKII or FLAG-cGKII KD plasmid and affinity-purified these proteins using anti-FLAG columns (Fig. 5B). We observed that cGKII WT but not KD specifically phosphorylated GST-FoxO1 in the presence of cGMP (Fig. 5C), and that cGKII targeted at least two sites of FoxO1, which were in FoxO-N and FoxO-C (Fig. 5A and D). A previous report has shown that cGKIα phosphorylates the human FoxO1 forkhead domain mainly at S152–155 and S184, by which the DNA-binding activity of FoxO1 is abolished [22]. We found that cGKII also phosphorylates FoxO1 at S152–155 and that these residues are major sites of phosphorylation in FoxO-N (Fig. S5A and B). However, the replacement of serine with alanine at S152–155 had little effect on the FoxO-transcriptional stimulation by cGKII and the binding to 14-3-3ε protein, which regulates the cytosolic localization of FoxO, in this context (Fig. S5C and D). Next, we determined phosphorylation sites in FoxO-C. Experiments with several truncated FoxO1 mutants narrowed down the phosphorylation sites in FoxO-C and identified S319 as a major phospho-residue targeted by cGKII (Fig. 5E and F). We also confirmed that overexpression of cGKII in the presence of 8-Br-cGMP stimulates the phosphorylation of the FoxO1 S319 site in human cultured cells (Fig. 3D, lane 2). Although cGKIα also phosphorylated GST-tagged full-length FoxO1 *in vitro*, the S319 site did not appear to be a major phosphorylation site (Fig. S6). The S319 site was also targeted by LRRK2 as shown previously (Fig. 5F) and co-incubation of cGKII and LRRK2 enhanced phosphorylation of the FoxO-C fragment in *in vitro* kinase assays (lane 5 compared with lane 1 in Fig. 5G). In contrast to the phosphorylation of FoxO at S152 155, the replacement of serine with alanine at S319 suppressed FoxO-transcriptional activity and abolished cGKII-mediated stimulation of FoxO, suggesting that phosphorylation at S319 has a major effect on the activity mediated by cGKII as well as LRRK2 (Fig. 4C) [16].

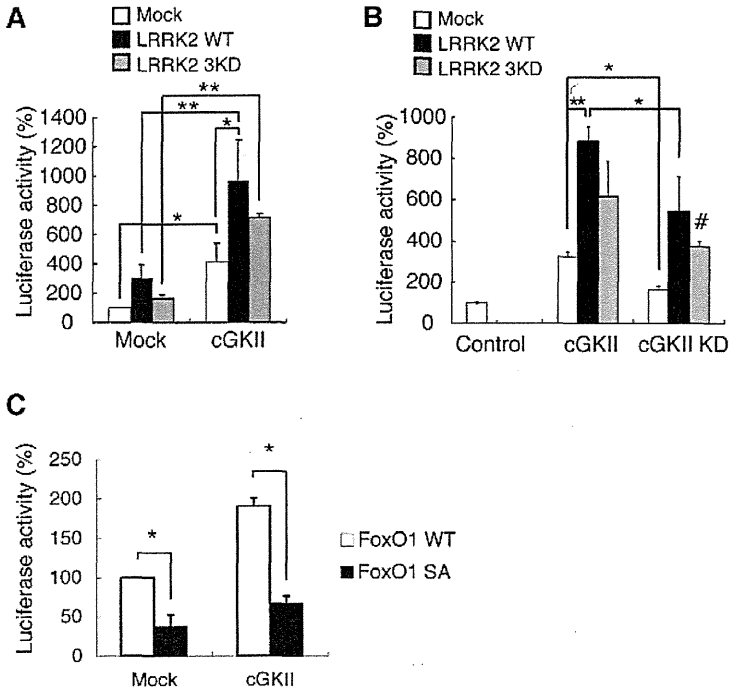

Figure 4. cGKII stimulates FoxO-transcriptional activity. (A, B) cGKII and LRRK2 additively stimulate FoxO-transcriptional activity. FoxO-transcriptional activity was measured in extracts prepared from 293T cells transfected with the indicated plasmids and a plasmid for FoxO1, a FoxO reporter plasmid containing *Firefly* luciferase, and a plasmid for *Renilla* luciferase to monitor the transfection efficiency. The relative FoxO-transcriptional activity (*Firefly* luciferase activity) normalized to *Renilla* luciferase activity is presented. Data are presented as the mean ± SE for three independent experiments. β-galactosidase (Mock) served as a transfection control. **(C)** Introduction of the S319A (SA) mutation in FoxO1 reduced FoxO activity. Data are presented as the mean ± SE for three independent experiments. *, $p<0.05$; **, $p<0.01$. Co-transfection of kinase-dead forms of cGKII and LRRK2 also sitmulated FoxO (#, $p<0.05$ *vs.* Control in **B**).
doi:10.1371/journal.pone.0030958.g004

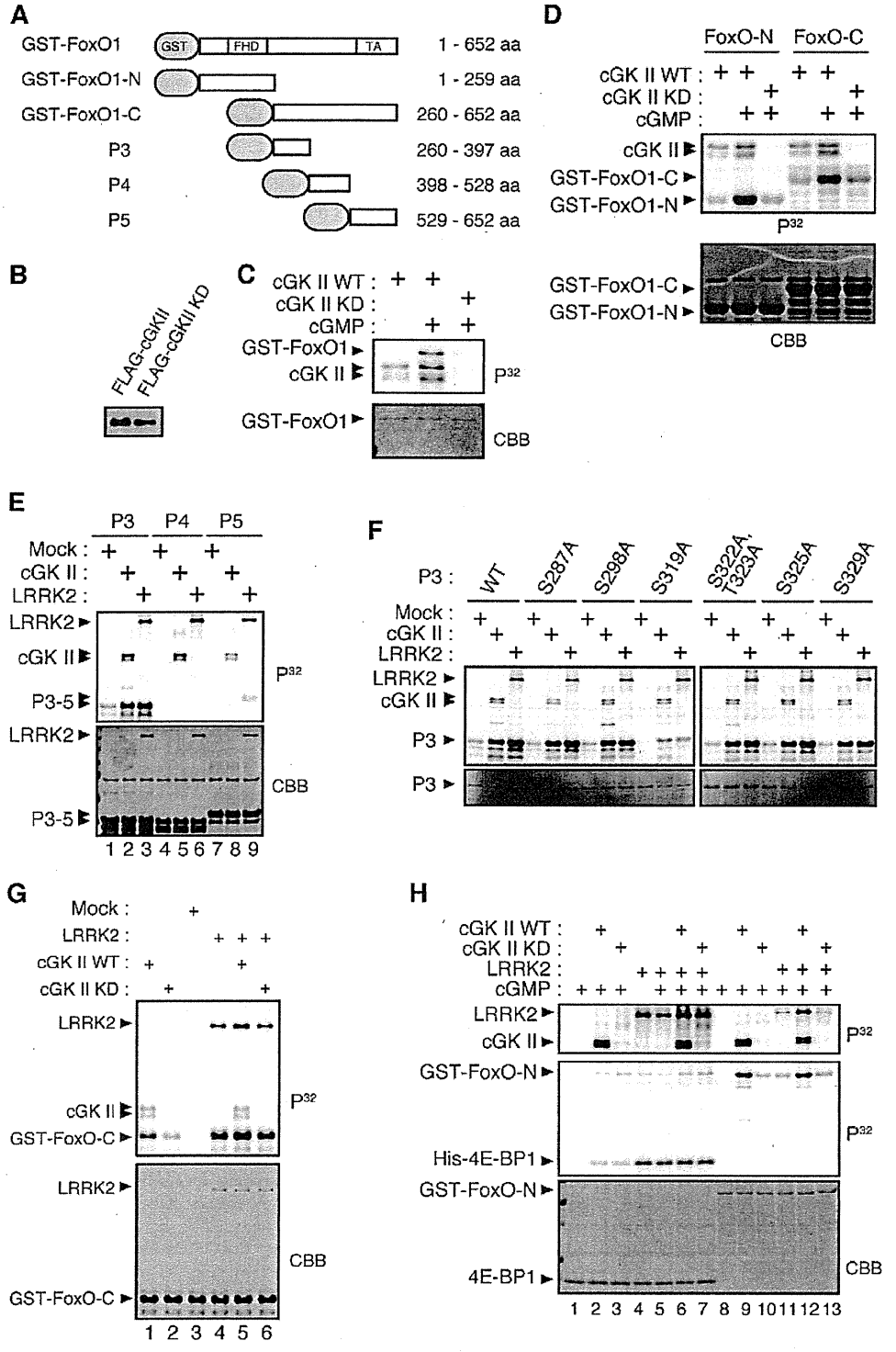

Figure 5. cGKII phosphorylates FoxO1 *in vitro*. (**A**) The recombinant FoxO1 proteins used as substrates. GST, GST-tag. Numbers indicate corresponding amino acid residues of FoxO1. (**B**) FLAG-tagged cGKII and FLAG-cGKII KD were immunoprecipitated from FLAG-tagged cGKII or FLAG-cGKII KD-transfected 293T cells as kinase sources. Western blotting confirmed that the amounts of the two proteins obtained were similar. (**C, D**) *In vitro* kinase assays of cGKII using recombinant GST-FoxO1 as a substrate. In the presence of cGMP, cGKII WT but not cGKII KD phosphorylated GST-FoxO, GST-FoxO-N, and GST-FoxO-C. Autoradiography (P^{32}) and Coomassie brilliant blue (CBB) staining of the gels are shown. Note cGKII proteins by

CBB staining were difficult to detect in spite of the presence of autophosphorylation signals of cGKII (cGKII in P^{32}) (**E**) cGKII and LRRK2 phosphorylated the P3 but not P4 or P5 protein. Autophosphorylation signals of cGKII and LRRK2 are also shown (cGKII and LRRK2 in P^{32}). The mock immunoprecipitate (Mock) served as a control. (**F**) *In vitro* kinase assay using P3 and a series of P3 mutants where the candidate phosphorylation residues are replaced with alanine (refer to [16] for information on the mutated residues). The phosphorylation by cGKII or LRRK2 was decreased in the P3 S319A mutant. (**G**) Co-incubation of cGKII and LRRK2 enhanced GST-FoxO-C phosphorylation. (**H**) cGKII failed to stimulate LRRK2 kinase activity and LRRK2 failed to stimulate cGKII kinase activity. His-tagged 4E-BP1 and GST-FoxO-N served as LRRK2-specific and cGKII-specific substrates, respectively.

doi:10.1371/journal.pone.0030958.g005

cGK phosphorylates LRRK2, but does not affect the kinase activity of LRRK2 in vitro

To examine the possibility that cGKII activates the kinase activity of LRRK2, or that LRRK2 activated cGKII, we further performed *in vitro* kinase assays using 4E-BP1 and FoxO-N as substrates (Fig. 5H). As reported [14], LRRK2 specifically phosphorylated 4E-BP1, which is not dependent on cGMP, while cGKII failed to do so (lanes 4 and 5 compared with lane 2 in Fig. 5H). cGKII and cGKII KD had little effect on the kinase activity of LRRK2 toward 4E-BP1 (lanes 6 and 7 *vs.* lanes 4 and 5 in Fig. 5H). cGKII but not cGKII KD or LRRK2 effectively phosphorylated FoxO-N (lane 9 compared with lanes 10 and 11 in Fig. 5H). Again LRRK2 had little effect on the kinase activity of cGKII toward FoxO-N (lane 12 compared with lanes 9 and 13 in Fig. 5H). However, cGKII also appeared to phosphorylate LRRK2 without modifying the kinase activity of LRRK2 (lane 6 *vs.* lanes 5, and lane 12 *vs.* lane 11 in Fig. 5H and Fig. S7). The *in vitro* observation that cGKII and LRRK2 act independently was consistent with the results of the genetic test (Fig. 2) and the reporter assay (Fig. 4).

Phosphorylation of FoxO by DG2 as well as dLRRK causes DA neurodegeneration

We next examined the pathological consequence of the phosphorylation of FoxO by DG2 and dLRRK in *Drosophila*. Ubiquitous or pan-neuronal expression of DG2 or dFoxO using GAL4 drivers for constitutive expression caused death. We then employed the mifepristone-inducible GAL4 system (GeneSwitch-GAL4) that drives the tissue-specific expression of upstream activating sequence (UAS)-constructs in post-mitotic cells. Pan-neuronal co-expression of dFoxO with DG2, but not the expression of either dFoxO or DG2 alone, caused significant neuronal loss in the PPM1/2 cluster Tyrosine hydroxylase (TH)-positive neurons of the adult brain (Fig. 6A). Expression of dLRRK I1915T exacerbated the neurotoxicity mediated by dFoxO and DG2 co-expression (Fig. 6A). In this context, the introduction of the S259A mutation, which corresponds to S319A in human FoxO1, attenuated the toxic interaction of dFoxO with DG2 (Fig. 6B). Consistent with the viability of TH-positive neurons, the motor activity of the flies expressing dFoxO and DG2 was impaired (Fig. 6C). Co-expression of dLRRK I1915T further worsened the motor dysfunction (Fig. 6C). Treatment with 1 mM L-3,4-dihydroxyphenylalanine (L-DOPA) significantly improved the locomotor activity of dFoxO and DG2-coexpressing flies (Fig. 6D), suggesting that the reduction in motor activity reflects DA degeneration. The expression of only DG2 mildly affected lifespan (Fig. 6E), whereas the co-expression of DG2 and dFoxO significantly shortened lifespan (Fig. 6E). However, the dFoxO S259A mutation failed to suppress the decrease in lifespan caused by the co-expression of dFoxO and DG2, suggesting that the toxic interaction of DG2 with dFoxO that affects lifespan is produced by a different mechanism rather than phosphorylation at S259 by DG2 (Fig. 6F). We then examined whether endogenous dFoxO contributes to DG2-mediated toxicity in *Drosophila* (Fig. 7A and B). Pan-neuronal expression of DG2 alone by the GeneSwitch-GAL4 driver caused mild motor defect (Fig. 7A). Removal of one copy of functional FoxO allele had little effect on the motor function (Fig. 7A) and lifespan (Fig. 7B) whereas it partly suppressed DG2-mediated motor dysfunction (Fig. 7A) and reduction in lifespan (Fig. 7B). These results suggested that endogenous dFoxO is also involved in neurodegeneration by DG2.

NO signal leads to DA neurodegeneration through DG2-FoxO

The activation of cGK requires cGMP. cGMP is generated by the NO-mediated activation of sGCs as well as ligands-mediated activation of receptor GCs [23,24,25]. However, as NO generated by NOS has been implicated in PD, the role of NOS-sGC was investigated via functional assays in *Drosophila*. We tested whether the *Drosophila* NO signal components dNOS and sGC are indeed involved in FoxO and DG2-mediated DA neurodegeneration in *Drosophila* (Fig. 8). Genetic interaction tests showed that co-expression of dNOS enhances the FoxO-mediated degeneration in the eye (Fig. 8B). In contrast, knockdown of sGC α or β subunits partially improved the phenotype of dFoxO expression (Fig. 8C and D). Moreover, knockdown of sGCα or removal of one copy of the DG2 genes improved the eye degeneration caused by co-expression of dFoxO with dNOS (Fig. 8E and F compared with B). In the context of pan-neuronal expression of FoxO and DG2 in *Drosophila*, treatment with a NOS inhibitor, Nω-Nitro-L-Arginine-Methyl-Ester (L-NAME), but not the inactive D-enantiomer D-NAME, significantly suppressed loss of the PPM1/2 and PPL1 cluster DA neurons (Fig. 9A E). In this setting, L-NAME treatment specifically reduced phosphorylation of dFoxO (Fig. 9F). The endogenous function of dNOS-DG2 signaling in DA neurodegeneration was estimated by survival assays of DG2 or dNOS mutant flies administrated with a PD-related toxin, paraquat, where both mutant lines showed significant resistances to paraquat (Fig. 9G). These results suggested that DG2/cGKII activated by NO signal could affect the survival of DA neurons through FoxO.

Discussion

We have previously demonstrated that dLRRK/LRRK2 phosphorylates and stimulates FoxO, which confers neurotoxic activity to FoxO, activating the expression of pro-apoptotic proteins such as Bim/Hid [16]. Searching for LRRK2-FoxO signaling components, we found that *Drosophila* cGK DG2 also exacerbates FoxO-mediated neurotoxicity. The current study suggests that cGKII/DG2 activates FoxO similar to, but independently of, LRRK2. However, in spite of the similar activation mechanism, the genetic results suggested that the Hid-DIAP-Drone pathway is not a major cause of the optic degeneration by DG2-FoxO (Fig. S8A–D). Supporting this result, a quantitative RT-PCR analysis showed that DG2 or DG2/dFoxO does not effectively stimulate FoxO-mediated transactivation of *hid* as well as *4E-BP* (Fig. S8E and F). We attempted to determine downstream effector(s) of DG2-dFoxO using a combination of microarrays, real-time PCR and *Drosophila* genetic screening, but could not identify any candidate genes, suggesting

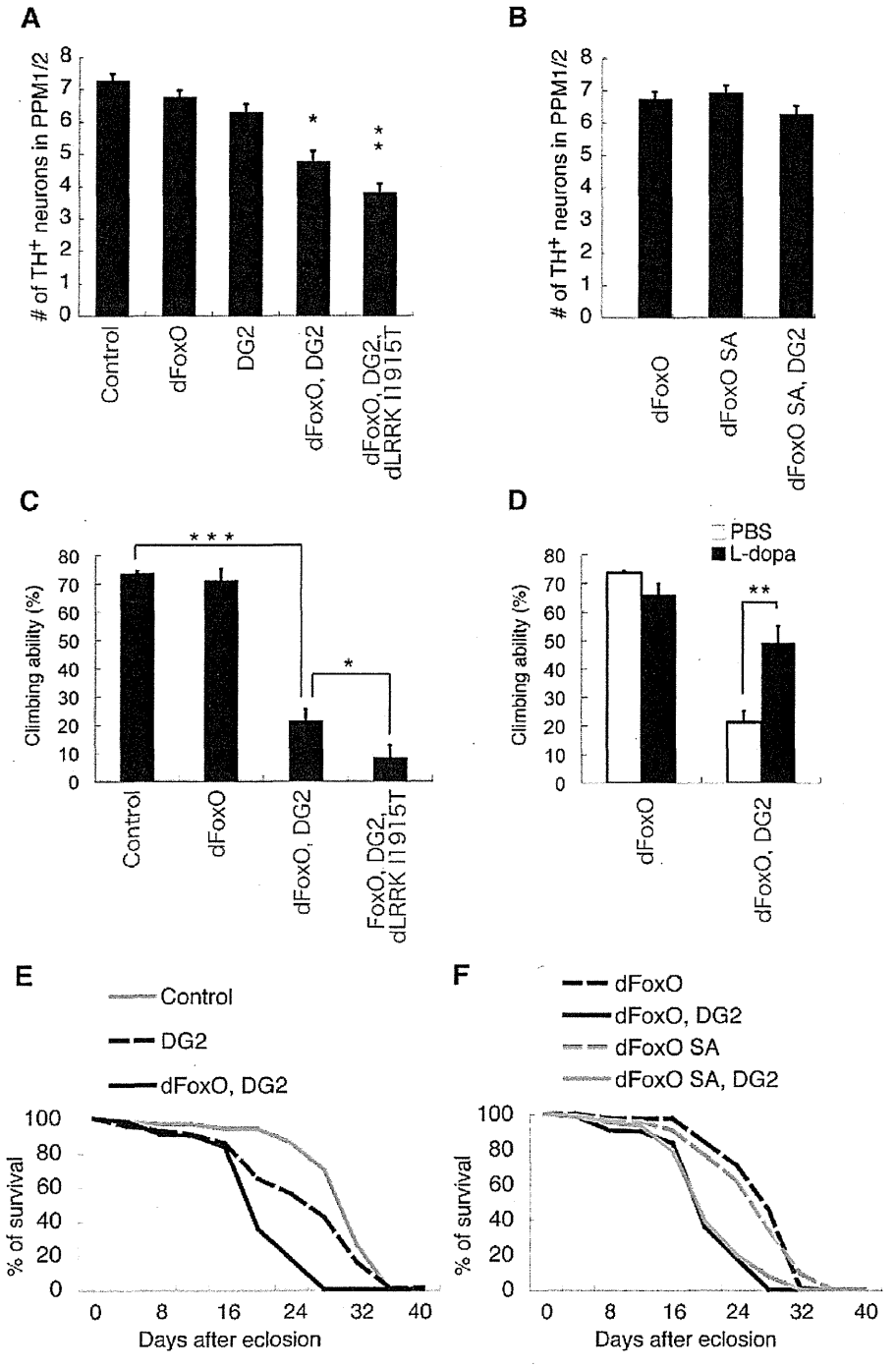

Figure 6. Neuronal activation of dFoxO by DG2 affects the maintenance of DA neurons in *Drosophila*. **(A)** The number of protocerebral posterior medial (PPM) 1/2 clusters of Tyrosine hydroxylase (TH)-positive DA neurons in 24-day-old adult flies. Neuron-specific expression of dFoxO, dLRRK I1915T and/or DG2 was induced following the administration of the activator RU486 (25 μg/mL) in the *elav-GeneSwitch-GAL4* (*elav-GS*) crosses. *elav-GS/+* served as a control. Data are presented as the mean ± SE for three repeated experiments (*, $P<0.05$; **, $p<0.01$). **(B)** Co-expression of the dFoxO S259A (SA) mutant with DG2 suppressed the loss of PPM 1/2 TH-positive neurons. Flies were treated as in **(A)**. **(C)** Adult aged flies expressing dFoxO and DG2 under the control of *elav-GS* showed motor defects, while the expression of dFoxO alone had little effect. The values represent means ± SE for 20 trials in six independent experiments (*, $p<0.05$; ***, $p<0.001$). **(D)** Treatment with 1 mM L-DOPA in phosphate-buffered saline (PBS), but not with PBS alone, for 4 days rescued the loss of climbing ability in dFoxO and DG2-expressing flies. dFoxO served as a control. The values represent means ± SE for 20 trials in six independent experiments (**, $p<0.01$). **(E)** Flies from each genotype were subjected to survival assays

at 29μC. *elav-GS/+* served as a control. Female adults ($n=119–121$) were fed yeast paste containing 25 μg/mL RU486. Expression of DG2 shortened lifespan compared with the control (DG2 *vs.* Control, $p<0.01$; dFoxO, DG2 *vs.* Control, $p<0.0001$). (**F**) Flies from each genotype ($n=119–122$) were subjected to survival assays as in (**E**). Pan-neuronal expression of dFoxO SA alone had no significant effect on lifespan when compared with that of dFoxO. Co-expression of dFoxO SA with DG2 failed to attenuate the effect of dFoxO-DG2 combination on lifespan (dFoxO SA, DG2 *vs.* dFoxO, DG2; $p=0.485$).
doi:10.1371/journal.pone.0030958.g006

that DG2 has more complex functions in gene regulation. For example, DG2 might modulate another transcription regulator through phosphorylation along with dFoxO.

Activation of the NOS-sGC pathway leads to increased cGMP levels [26], which in turn has physiological consequences by regulating cGMP effector proteins such as cGMP-regulated ion channels, cGMP-regulated phosphodiesterases, and cGKs [25,27]. It is widely appreciated that cGKs have a variety of roles in tissues, and in the central nervous system. For instance, cGKs regulate neurotransmitter release/uptake and receptor trafficking, neuronal differentiation and axon guidance, synaptic plasticity and memory through the phosphorylation of substrates [27,28,29]. There are two cGK isoforms, cGKI α/β and cGKII, in vertebrates. While cGKI α/β is cytosolic and mainly found in the cerebellum, cerebral cortex, hippocampus, hypothalamus, and olfactory bulb of the brain, cGKII is located in the cellular membranes and widely distributed in the brain [30,31,32]. Here, we demonstrated that cGKII is abundantly expressed in DA neurons in the substantia nigra of the murine midbrain, suggesting that cGKII has a pathogenic role similar to DG2.

What signal mediates stimulation of cGMP synthesis and subsequent cGKII activation in PD remains unclear. The activation of microglia is believed to be one of the pathological processes [33,34], which might begin with the release of aggregated proteins such as oligomeric α-synuclein from neurons into the extracellular space [35]. Inflammation will be amplified by microglial activation and the release of proinflammatory cytokines and inducible NOS [5]. Similarly, dNOS, the only NOS orthologue in *Drosophila*, is involved in an immune response [36]. Thus, inducible NOS responding early to inflammation could be a trigger of the cGKII-FoxO-mediated neurotoxic pathway in humans. In this context, pathogenic LRRK2 with increased kinase activity might potentiate the above pathogenic mechanism. We found that cGKII physically interacts with LRRK2 (Fig. S9), and that they are co-localized at the endosomes (Fig. S10) although our current study suggests LRRK2 and cGKII act independently in the context of FoxO activation. However, we observed that co-expression of cGKII KD and LRRK2 3KD partially stimulates FoxO (Fig. 4B). These kinases have been reported to form a dimmer when activated [29,37,38]. Thus overexpression of kinase-dead forms of cGKII and LRRK2 may accidentally recruit and activate the endogenous kinases in 293T cells although we could not detect the endogenous expression of cGKII in this cell line.

The involvement of NO signaling in PD has been suggested by the findings of higher levels of nNOS and iNOS in the nigrostriatal region and basal ganglia in post mortem PD brains [3,4]. The emerging evidence for pathogenic roles of microglia and astrocytes in PD now supports the idea that glia-induced inflammation and NO production promote the disease's development. However, most studies with post mortem samples or PD models showed only that NO could be a generator of oxidative stress since NO is a free radical involved in a wide range of physiologic events [39]. A very recent study on rodent models of PD have shown that specific inhibition of sGC-cGMP signaling improves basal ganglia dysfunction and motor symptoms, suggesting that NO signaling could act specifically on PD etiology [40]. Our study here provides the possibility that NO signaling downstream to cGK along with FoxO has a pathogenic role in PD.

The relationship between the NO signal and FoxO has been pointed out in a report on a tail suspension-induced model of muscle atrophy, where nNOS-NO is suggested to induce muscle atrophy by upregulating the muscle-specific E3 ubiquitin ligases MuRF-1 and atrogin-1/MAFbx through FoxO activation. Since, the AKT signal is not involved in this mechanism, the molecular mechanism by which FoxO is regulated by nNOS-NO remains unknown [41]. Considering our finding regarding neurodegeneration, cGK may regulate FoxO as a mediator of the NO signal in the atrophic muscles as well. Studies have shown that cGK

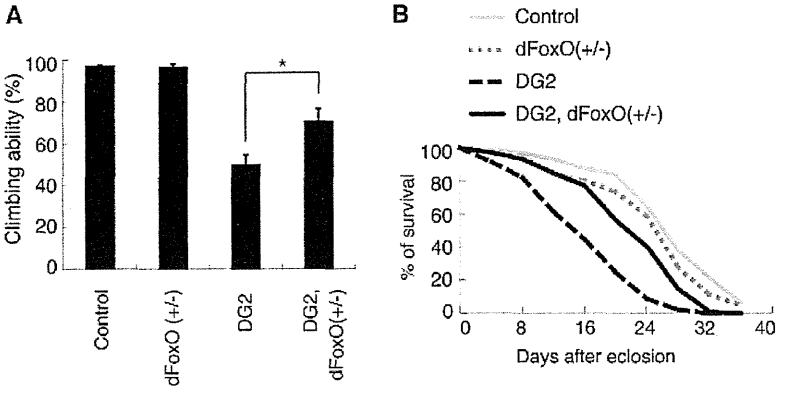

Figure 7. Reduction of endogenous dFoxO activity suppresses DG2-mediated toxicity. (**A**) The climbing activity was measured as in Figure 6C. The values represent means ± SE for 20 trials in three independent experiments (*, $p<0.05$). (**B**) Survival assays of female adults ($n=105–106$) were performed as in Figure 6E. DG2 *vs.* DG2, dFoxO (+/−), $p<0.01$; DG2, dFoxO (+/−) *vs.* Control, $p<0.01$. The genotypes are: *elav-GS/+* (Control), *UAS-DG2; elav-GS* (DG2), *elav-GS/dFoxO*^{21} (dFoxO (+/−)), *UAS-DG2; elav-GS/dFoxO*^{21} (DG2, dFoxO (+/−)).
doi:10.1371/journal.pone.0030958.g007

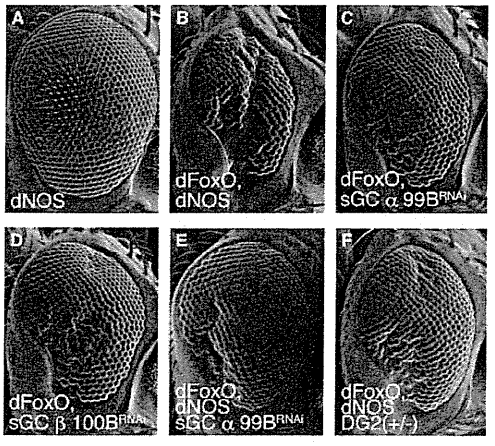

Figure 8. NO signal is involved in FoxO-mediated neurodegeneration. (A–D) SEM images of the eyes of flies expressing the indicated genes. The genotypes are: *GMR-Gal4/UAS-dNOS* **(A)**, *GMR-Gal4, UAS-dFoxO/UAS-dNOS* **(B)**, *GMR-Gal4, UAS-dFoxO; UAS-sGCα99B^{RNAi}* **(C)**, *GMR-Gal4, UAS-dFoxO; UAS-sGCβ100B^{RNAi}* **(D)**, *GMR-Gal4, UAS-dFoxO/UAS-dNOS; UAS-sGCα99B^{RNAi}* **(E)**, *GMR-Gal4, UAS-dFoxO/UAS-dNOS, DG2^{k04703}* **(F)**.
doi:10.1371/journal.pone.0030958.g008

indirectly activates FoxO4 through activation of the JNK pathway [42,43], which provides anti-tumor effects in colon cancer cells. Although the proposed sites of phosphorylation by JNK do not appear to be conserved in dFoxO, there is substantial evidence that JNK-FoxO regulates different cellular processes including anti-aging and cell death in *Drosophila* [44,45,46]. Thus, DG2 could also stimulate the JNK pathway in conjunction with FoxO, widely affecting a variety of cellular mechanisms. This idea could explain why the FoxO SA mutant failed to suppress the DG2-mediated decrease in lifespan of *Drosophila* (Fig. 6E and F).

Although more studies are needed in mammalian systems, our finding of a novel link between the NO signal and FoxO in neurodegeneration suggests that appropriate pharmacological control of the NO pathway would prevent or diminish pathological problems in PD.

Materials and Methods

Drosophila genetics

The *Drosophila* cultures and crosses were performed on standard fly food containing yeast, cornmeal and molasses, and flies were raised at 25uC unless otherwise stated. General fly stocks and *GAL4* lines were obtained from the Bloomington *Drosophila* stock center. These flies have been described previously: *UAS-dFoxO* [47], *UAS-dFoxO S259A* [16], *UAS-DG1* [18], *UAS-DG2* [18], *UAS-dNOS* [48], *UAS-hLRRK2 WT* [49], *UAS-hLRRK2 I2020T* [49], *UAS-dLRRK WT* [14], *UAS-dLRRK I1915T* [14], *UAS-dLRRK 3KD* [14], *e03680* (*dLRRK null*) [14], *elav*-GeneSwitch [50], *UAS hipo/MST* [51], *UAS-dIKKβ* [52], *UAS-CKIα RNAi* [53], *dFoxO^{21}* [54], *dNOS$^{\Delta 15}$* [55], *UAS-AKT1* (Bloomington stock #8191), *UAS-CDK1-Myc* (#6642), *UAS-CDK2-Myc* (#6634), *UAS-bsk/JNK* (#6407), *mnb^{EY14320}/DYRK1^{EY14320}* (#21430), *CkIα^{EP1555}* (#17009, [56]), *DG2^{k04703}* (#10382), *UAS-sGCα99B^{RNAi}* (#28748), *UAS-sGCβ100B^{RNAi}* (#28786), *hid^{I}* (#631), *DIAP^{1}* (#618), and *UAS-Dronc ^{RNAi}* (NIG-fly 8091R-2 III). *UAS-human cGKII* was generated in the Davies lab.

Antibodies

The anti-α-Tubulin (DM1A), anti-β-Tubulin (Tub2.1) and anti-FLAG (M2) antibodies were purchased from Sigma-Aldrich. The anti-FoxO1 (#9454) antibody was obtained from Cell Signaling Technology. The anti-Myc (4A6), anti-Actin (MAB1501) and anti-phospho-FoxO1 (Ser319, 51136-1) antibodies were purchased from Millipore, Chemicon and Signalway, respectively. The rabbit anti-*Drosophila* TH and anti-dFoxO polyclonal antibody has been described previously [16,57]. Anti-cGKII [30] and anti-cGKIα [31] were kindly provided by Drs. M. Hoffmeister and P. Weinmeister, respectively. The rabbit anti-hLRRK2 polyclonal antibodies were raised against GST-hLRRK2 (823–1004 aa) and (1868–2138 aa) produced in *E. coli* BL21(DE3)pLysS (Novagen).

Plasmids

cDNA for human cGKIα and rat cGKII, kindly provided by Drs. S. Lohmann and A. Smolenski, was subcloned into pcDNA3-Myc or pcDNA3-FLAG. A plasmid for EGFP-FoxO1 was a kind gift from Dr. T. Unterman. A plasmid for AKT-PH-GFP was from Addgene. Plasmids for *FLAG-hLRRK2* and *FLAG-dLRRK* [14], mouse FoxO1, and human 4E-BP1 and the luciferase reporter plasmid for FoxO (TK.IRS3) have been reported elsewhere [58]. The plasmid for DG2 was also reported previously [18]. Mutations were introduced using the QuikChange II XL Site-directed mutagenesis kit (Stratagene). Although we used mouse FoxO1 cDNA as a mammalian FoxO gene, the numbering is based on the human sequence to avoid confusion. Thus, Ser149–152, Ser181 and Ser316 in mouse FoxO1 correspond to Ser152–155, Ser184 and Ser319 in human FoxO1, respectively. The kinase-dead form of rat cGKII (cGKII KD) was generated by replacing Asp549 with alanine, which corresponds to bovine cGKIα D501A mutation described in [59].

In vitro phosphorylation assay

FLAG-cGKII, FLAG-hLRRK2, and mock fractions immunopurified from transfected and mock-transfected 293T cells were used as kinase sources. The same batches of kinase fractions were used throughout the experiments, and their quality and quantity was confirmed by western blot as shown in Fig. 5B and S6. Five micrograms of GST-FoxO1, mutant forms of GST-FoxO1 and His-4E-BP1 were incubated with the kinase sources in a kinase reaction buffer containing 20 mM HEPES (pH7.4), 15 mM $MgCl_2$, 5 mM EGTA, 0.1% Triton X-100, 0.5 mM DTT, 1 mM β-glycerolphosphate, and 2.5 μCi [γ-^{32}P]-ATP in the presence or absence of 30 μM cGMP for 30 min at 30uC. The reaction mixture was then suspended in SDS sample buffer and subjected to SDS-PAGE and autoradiography.

Cell culture, immunopurification and western blotting

Transfection of human embryonic kidney 293T and *Drosophila* Schneider 2 (S2) cells, immunopurification from the transfected cell or mouse brain lysate, and western blotting were performed as described previously [16,60,61]. Flp-In T-REx-293 cell line

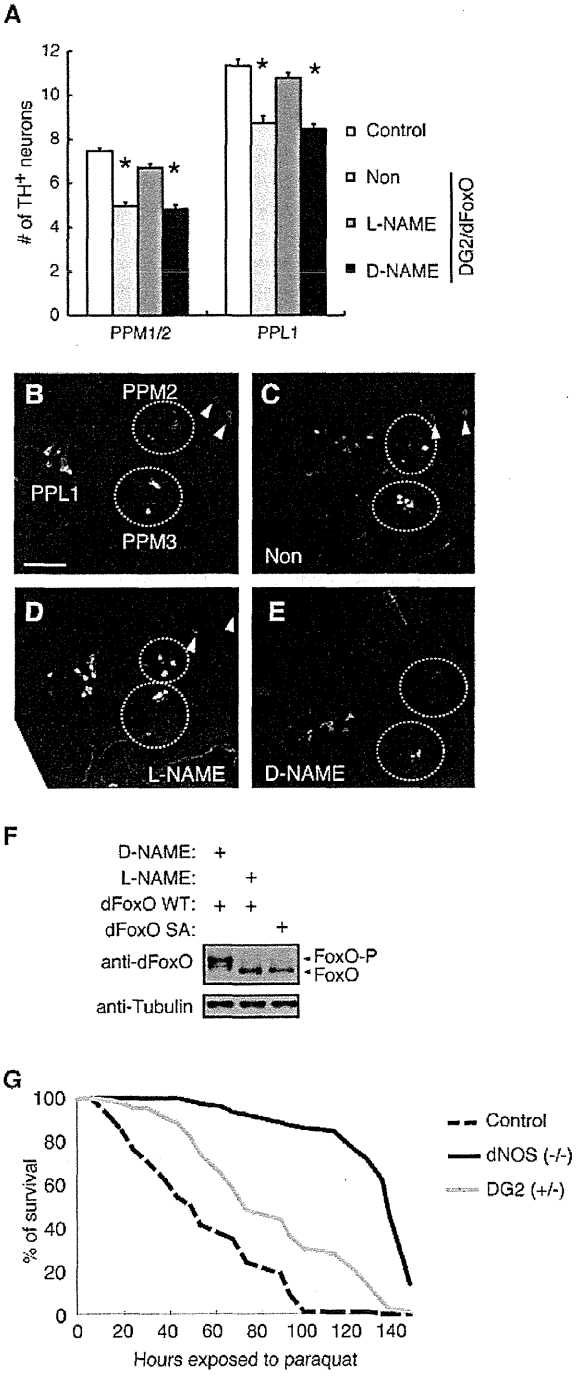

Figure 9. Inhibition of NO signal improves DG2-dFoxO-mediated DA neurodegeneration. **(A)** Newly eclosed normal *w-* flies (*Control*) or transgenics harboring *elav-GS>UAS-dFoxO/UAS-DG2* ($n=22$ in each) were fed a yeast paste containing 50 μg/mL_ RU486 with or without 10 mM L-NAME or D-NAME every 4 days at 29uC. The graph presents the number of PPM 1/2 and PPL1 clusters of TH-positive neurons in 20-day-old adult flies. PPM1 and PPM2 clusters were counted together. Data are presented as the mean ± SE for three experiments (*, $p<0.05$ *vs.* Control). PPL, the protocerebral posterior lateral. Non; RU486 only. **(B)** A representative image of TH-positive PPL1, PPM1, PPM2 (upper circle) and PPM3 (lower circle) neurons of a wild-type *w-* adult fly. Arrowheads indicate a pair of PPM1 neurons. Bar=50 μm. **(C–E)** Representative images of TH-positive neurons treated as in **A**. **(F)** Brain tissues of dFoxO transgenic flies treated with L-NAME or D-NAME were subjected to western blot analysis with anti-dFoxO. dFoxO SA mutant was also included as a non-phosphorylated *control*. Transgenes were expressed by the *elav-GS driver*. **(G)** Reduction of dNOS and DG2 activities confers stress resistance against 2 mM paraquat treatment. dNOS (−/−) *vs.* Control, $p<0.0001$; DG2 (+/−) *vs.* Control, $p<0.01$. The genotypes are: *w-* (Control), $dNOS^{\Delta 15}/dNOS^{\Delta 15}$ (dNOS (−/−)), $DG2^{k04703}$/+ (DG2 (+/−)).
doi:10.1371/journal.pone.0030958.g009

harboring doxycycline-inducible EGFP-FoxO1 gene was generated according to the manufacturer's instructions (Invitrogen).

Scanning Electron Microscopy (SEM)

Adult flies were processed as described previously [14]. SEM images were obtained at The Biomedical Research Core of Tohoku University Graduate School of Medicine.

Lifespan and survival assays

Twenty female adult flies per vial were maintained at 29uC, transferred to fresh fly food vials containing 250 μl of yeast paste and 25 μg/ml of RU486, and scored for survival every 4 days. To control for isogeny, all fly lines were backcrossed to the w^- wild-type background for six generations or were generated on the w^- background, and thus have matched genetic backgrounds. Survival assays of flies treated with 2 mM paraquat were performed as described previously [14].

Climbing assay

The climbing assay was performed as described previously [14]. Briefly, twenty flies were placed in a plastic vial (18.6 cm in height6 3.5 cm^2 in area) and gently tapped to bring them down to the bottom of the vial. Flies were given 18 s to climb and the number of flies more than 6 cm from the bottom was counted. Twenty trials were performed for the same set of flies. Flies at 20 days of age were left untreated or treated with 1 mM L-DOPA for 4 days, then subjected to climbing assays.

Whole-mount immunostaining

Total number of TH-positive neurons were calculated following whole-mount immunostaining of brain samples as described previously [57]. All immunohistochemical analyses were performed using a Carl Zeiss laser scanning microscope system.

Statistical analysis

The one-way repeated measures ANOVA was used to determine significant differences between multiple groups unless otherwise indicated. If a significant result was achieved ($p<0.05$), the means of the control and the specific test group were analyzed using the Tukey-Kramer test. For lifespan assays, a Kaplan-Meier analysis with the log-rank test was performed.

Supporting Information

Figure S1 Evaluation of mnb and dgl expression in $mnb^{EY14320}$ and UAS-DG1 fly lines in the presence of the GAL4 driver. Total RNA was extracted from the *Da-Gal4* crosses. The *mnb*, an orthologue of mammalian *DYRK1*, *dgl* and *rp49* transcript levels were measured by real-time PCR. *mnb* (A) or *dgl* (B) transcript levels normalized to those of *rp49* are presented. (TIF)

Figure S2 DG1 does not exacerbate dFoxO-mediated eye degeneration. Transgenic expression of DG2 alone did not produce eye degeneration, and DG1 had little effect on the eye phenotype caused by expression of dFoxO (when compared to Figure 2B). (C) The numbers of ommatidia per fly eye (from 5 flies) were quantified. *, $p<0.05$; N.S., non-significant. The genotypes are: *UAS-DG2; GMR-Gal4* (A), *GMR-Gal4, UAS-dFoxO; UAS-DG1* (B), *GMR-Gal4/UAS-EGFP* (EGFP), *GMR-Gal4, UAS-dFoxO/UAS-EGFP* (dFoxO, EGFP), *GMR-Gal4, UAS-dFoxO; UAS-DG1* (dFoxO, DG1) (C).
(TIF)

Figure S3 cGKII does not form a stable complex with cGKIα or FoxO1. Lysate from 293T cells transfected with cGKII-FLAG together with or without FoxO1-Myc or cGKIα-Myc was immunoprecipitated with anti-FLAG antibody (FLAG-IP). Immunoprecipitates and total soluble lysates (Lysate) were analyzed by western blotting.
(TIF)

Figure S4 cGKII is expressed in DA neurons of the murine midbrain. Immunolocalization of cGKIα (green in A, C), cGKII (green in B, D) and TH (red) in coronal sections of the substantia nigra (A, B) and striatum (C, D) of the brain. Yellow in B indicates the expression of cGKII in TH-positive neuronal processes (arrow heads) as well as cell bodies (arrows). The right columns of each panel show high-magnification images of the boxes in the left columns. Scale bars = 20 μm.
(TIF)

Figure S5 Mutations of cGKII phosphorylation sites localized in FoxO1-N do not affect the FoxO-transcriptional activity. (A) Reported phosphorylation sites in FoxO1 by cGKI are depicted [22]. Phospho-resistant mutants, where the indicated Ser or Thr residues are replaced with alanine, are also shown. (B) The phospho-signal by cGKII was decreased in GST-FoxO-4M compared with GST-FoxO-N WT (lane 3 *vs.* lane 2), but was no longer decreased in GST-FoxO-5M (data not shown), suggesting that S184 is not a major phosphorylation site by cGKII. (C) The FoxO1 4M mutation had little effect on FoxO-transcriptional activity stimulated by cGKII and/or LRRK2. (D) Effects of the 4M mutation on physical interaction between FoxO1 and 14-3-3ε were estimated in 293T cells. FoxO1-Myc-6x His was pulled down with Ni-NTA beads from the lysate of cells expressing the indicated transgenes.
(TIF)

Figure S6 The Ser319 site of FoxO1 is not a major target of cGKI in vitro. *In vitro* kinase assay was performed as in Fig. 5. P3 SA; a P3 mutant in which the Ser319 residue is replaced with alanine. Autophosphorylation signals of cGKII and cGKI are also shown in the upper panel.
(TIF)

Figure S7 cGKII phosphorylates LRRK2. (A) cGKII WT but not cGKII KD phosphorylates LRRK2 3KD (lane 9) as well as LRRK2 WT (lane 6) in *in vitro* kinase assay. *In vitro* kinase assay was performed as in Fig. 5. (B) Western blot analysis with anti-FLAG indicates similar amounts of FLAG-LRRK2 WT and FLAG-LRRK2 3KD were used in the kinase assay.
(TIF)

Figure S8 Hid is not a major gene responsible for FoxO-DG2-mediated optic degeneration. Introduction of loss-of-function alleles of a pro-apoptotic gene *hid* (B) or anti-apoptotic *DIAP* (C), or knockdown of Dronc, a caspase downstream of Hid (D), had little effects on the eye phenotype by co-expression of dFoxO and DG2 (A). The genotypes are: *UAS-DG2; GMR-Gal4, UAS-dFoxO* (A), *UAS-DG2; GMR-Gal4, UAS-dFoxO; hid^{1}* (B), *UAS-DG2; GMR-Gal4, UAS-dFoxO; DIAP^{J}* (C), *UAS-DG2; GMR-Gal4, UAS-dFoxO; UAS-Dronc^{RNAi}* (D). (E) Real-time RT-PCR analysis for *hid* and *4E-BP* was performed using total RNA from S2 cells expressing the indicated gene combinations. Values are presented as the mean ± SE for three repeated experiments. *, $p<0.05$ *vs.* Control.
(TIF)

Figure S9 cGKII is associated with LRRK2. (A) Lysate from 293T cells transfected with FLAG-tagged LRRK2 with or without Myc-cGKII was immunoprecipitated with anti-FLAG antibody (FLAG-IP). Immunoprecipitates and total soluble lysates (lysate) were analyzed by western blotting. (B) The diagram represents LRRK2 and the mutants used to determine the cGKII-binding domain. Numbers in parentheses indicate corresponding amino acid residues of LRRK2. LRR, leucine-rich repeat; ROC, Ras in complex proteins; COR, C-terminal of Roc; Kinase, protein kinase domain; WD40, WD40 domain. (C) Immunoprecipitation-western blot analysis as in (A) revealed cGKII to be associated with LRRK2-C. (D) cGKII associates strongly with LRRK2-C_3, and weakly with LRRK2-C_1 and -C_2. (E) Endogenous interaction of cGKII but not cGKIα with LRRK2 in brain tissue. Mouse brain tissues were lysed as described [60], then the supernatant fractions were immunoprecipitated (IP) with anti-cGKII or anti-cGKIα antibodies. The co-precipitated LRRK2 was detected by western blotting using anti-LRRK2 antibody. 293T lysate expressing FLAG-LRRK2 or FLAG-cGKII served as a positive control.
(TIF)

Figure S10 cGKII is co-localized with LRRK2 at the endosomes. (A) Immunolocalization of cGKII and LRRK2 in 293T cells expressing FLAG-LRRK2 and Myc-cGKII. cGKII and LRRK2 were visualized with anti-Myc (green) or anti-LRRK2 antibody (red). LRRK2 is localized at the Rab-positive endosomes (data not shown). cGKII is localized at the cytoplasmic membrane and partly in the cytoplasmic compartments. cGKII and LRRK2 were co-localized at the Rab-positive endosomes (yellow). Scale bar = 10 μm. (B–E) Immunolocalization of cGKII (red) in 293T cells expressing Myc-cGKII and EGFP-tagged Rabs (green). Cytosolic cGKII is located mainly at Rab4- and Rab5-positive endosomes, and partially at Rab7- or Rab11-positive endosomes.
(TIF)

Acknowledgments

We thank A. Yasui, S. Nakajima, S. Kanno and M. Kaji for excellent technical support and equipment, and T. Furuyama, T. Unterman, G. Halder, K.V. Anderson, J. Jiang, T. Osterwalder S. Lohmann, A. Smolenski, M. Hoffmeister, F. Hofmann, P. Weinmeister, PH. O'Farrell and M. Fukuda for the generous supply of materials.

Author Contributions

Conceived and designed the experiments: TK YI. Performed the experiments: TK TS YI. Analyzed the data: TK YI. Contributed reagents/materials/analysis tools: TS SD HI KH RT NH. Wrote the paper: YI.

References

1. Steinert JR, Chernova T, Forsythe ID (2010) Nitric oxide signaling in brain function, dysfunction, and dementia. Neuroscientist 16: 435–452.
2. West AR, Tseng KY (2011) Nitric Oxide-Soluble Guanylyl Cyclase-Cyclic GMP Signaling in the Striatum: New Targets for the Treatment of Parkinson's Disease? Front Syst Neurosci 5: 55.
3. Hunot S, Boissiere F, Faucheux B, Brugg B, Mouatt-Prigent A, et al. (1996) Nitric oxide synthase and neuronal vulnerability in Parkinson's disease. Neuroscience 72: 355–363.
4. Eve DJ, Nisbet AP, Kingsbury AE, Hewson EL, Daniel SE, et al. (1998) Basal ganglia neuronal nitric oxide synthase mRNA expression in Parkinson's disease. Brain Res Mol Brain Res 63: 62–71.
5. Liberatore GT, Jackson-Lewis V, Vukosavic S, Mandir AS, Vila M, et al. (1999) Inducible nitric oxide synthase stimulates dopaminergic neurodegeneration in the MPTP model of Parkinson disease. Nat Med 5: 1403–1409.
6. Muramatsu Y, Kurosaki R, Watanabe H, Michimata M, Matsubara M, et al. (2003) Cerebral alterations in a MPTP-mouse model of Parkinson's disease an immunocytochemical study. J Neural Transm 110: 1129–1144.
7. Dreyer J, Schleicher M, Tappe A, Schilling K, Kuner T, et al. (2004) Nitric oxide synthase (NOS)-interacting protein interacts with neuronal NOS and regulates its distribution and activity. J Neurosci 24: 10454–10465.
8. Paisan-Ruiz C, Jain S, Evans EW, Gilks WP, Simon J, et al. (2004) Cloning of the gene containing mutations that cause PARK8-linked Parkinson's disease. Neuron 44: 595–600.
9. Zimprich A, Biskup S, Leitner P, Lichtner P, Farrer M, et al. (2004) Mutations in LRRK2 cause autosomal-dominant parkinsonism with pleomorphic pathology. Neuron 44: 601–607.
10. Healy DG, Falchi M, O'Sullivan SS, Bonifati V, Durr A, et al. (2008) Phenotype, genotype, and worldwide genetic penetrance of LRRK2-associated Parkinson's disease: a case-control study. Lancet Neurol 7: 583–590.
11. Mata IF, Wedemeyer WJ, Farrer MJ, Taylor JP, Gallo KA (2006) LRRK2 in Parkinson's disease: protein domains and functional insights. Trends Neurosci 29: 286–293.
12. West AB, Moore DJ, Biskup S, Bugayenko A, Smith WW, et al. (2005) Parkinson's disease-associated mutations in leucine-rich repeat kinase 2 augment kinase activity. Proc Natl Acad Sci U S A 102: 16842–16847.
13. Gloeckner CJ, Kinkl N, Schumacher A, Braun RJ, O'Neill E, et al. (2006) The Parkinson disease causing LRRK2 mutation I2020T is associated with increased kinase activity. Hum Mol Genet 15: 223–232.
14. Imai Y, Gehrke S, Wang HQ, Takahashi R, Hasegawa K, et al. (2008) Phosphorylation of 4E-BP by LRRK2 affects the maintenance of dopaminergic neurons in Drosophila. Embo J 27: 2432–2443.
15. Lessing D, Bonini NM (2009) Maintaining the brain: insight into human neurodegeneration from Drosophila melanogaster mutants. Nat Rev Genet 10: 359–370.
16. Kanao T, Venderova K, Park DS, Unterman T, Lu B, et al. (2010) Activation of FoxO by LRRK2 induces expression of proapoptotic proteins and alters survival of postmitotic dopaminergic neuron in Drosophila. Hum Mol Genet 19: 3747–3758.
17. Kalderon D, Rubin GM (1989) cGMP-dependent protein kinase genes in Drosophila. J Biol Chem 264: 10738–10748.
18. MacPherson MR, Lohmann SM, Davies SA (2004) Analysis of Drosophila cGMP-dependent protein kinases and assessment of their in vivo roles by targeted expression in a renal transporting epithelium. J Biol Chem 279: 40026–40034.
19. Jarchau T, Hausler C, Markert T, Pohler D, Vanderkerckhove J, et al. (1994) Cloning, expression, and in situ localization of rat intestinal cGMP-dependent protein kinase II. Proc Natl Acad Sci U S A 91: 9426–9430.
20. Kulaksiz H, Rehberg E, Stremmel W, Cetin Y (2002) Guanylin and functional coupling proteins in the human salivary glands and gland tumors: expression, cellular localization, and target membrane domains. Am J Pathol 161: 655–664.
21. Yuasa K, Yamagami S, Nagahama M, Tsuji A (2008) Trafficking of cGMP-dependent protein kinase II via interaction with Rab11. Biochem Biophys Res Commun 374: 522–526.
22. Bois PR, Brochard VF, Salin-Cantegrel AV, Cleveland JL, Grosveld GC (2005) FoxO1a-cyclic GMP-dependent kinase I interactions orchestrate myoblast fusion. Mol Cell Biol 25: 7645–7656.
23. Bicker G (2007) Pharmacological approaches to nitric oxide signalling during neural development of locusts and other model insects. Arch Insect Biochem Physiol 64: 43–58.
24. Davies S (2000) Nitric oxide signalling in insects. Insect Biochem Mol Biol 30: 1123–1138.
25. Davies SA (2006) Signalling via cGMP: lessons from Drosophila. Cell Signal 18: 409–421.
26. Wang X, Robinson PJ (1997) Cyclic GMP-dependent protein kinase and cellular signaling in the nervous system. J Neurochem 68: 443–456.
27. Hofmann F, Feil R, Kleppisch T, Schlossmann J (2006) Function of cGMP-dependent protein kinases as revealed by gene deletion. Physiol Rev 86: 1–23.
28. Feil R, Hofmann F, Kleppisch T (2005) Function of cGMP-dependent protein kinases in the nervous system. Rev Neurosci 16: 23–41.
29. Serulle Y, Zhang S, Ninan I, Puzzo D, McCarthy M, et al. (2007) A GluR1-cGKII interaction regulates AMPA receptor trafficking. Neuron 56: 670–688.
30. de Vente J, Asan E, Gambaryan S, Markerink-van Ittersum M, Axer H, et al. (2001) Localization of cGMP-dependent protein kinase type II in rat brain. Neuroscience 108: 27–49.
31. Feil S, Zimmermann P, Knorn A, Brummer S, Schlossmann J, et al. (2005) Distribution of cGMP-dependent protein kinase type I and its isoforms in the mouse brain and retina. Neuroscience 135: 863–868.
32. Geiselhoringer A, Gaisa M, Hofmann F, Schlossmann J (2004) Distribution of IRAG and cGKI-isoforms in murine tissues. FEBS Lett 575: 19–22.
33. McGeer PL, Itagaki S, Boyes BE, McGeer EG (1988) Reactive microglia are positive for HLA-DR in the substantia nigra of Parkinson's and Alzheimer's disease brains. Neurology 38: 1285–1291.
34. Glass CK, Saijo K, Winner B, Marchetto MC, Gage FH (2010) Mechanisms underlying inflammation in neurodegeneration. Cell 140: 918–934.
35. Roodveldt C, Christodoulou J, Dobson CM (2008) Immunological features of alpha-synuclein in Parkinson's disease. J Cell Mol Med 12: 1820–1829.
36. Foley E, O'Farrell PH (2003) Nitric oxide contributes to induction of innate immune responses to gram-negative bacteria in Drosophila. Genes Dev 17: 115–125.
37. Berger Z, Smith KA, Lavoie MJ (2010) Membrane localization of LRRK2 is associated with increased formation of the highly active LRRK2 dimer and changes in its phosphorylation. Biochemistry 49: 5511–5523.
38. Greggio E, Zambrano I, Kaganovich A, Beilina A, Taymans JM, et al. (2008) The Parkinson disease-associated leucine-rich repeat kinase 2 (LRRK2) is a dimer that undergoes intramolecular autophosphorylation. J Biol Chem 283: 16906–16914.
39. Aquilano K, Baldelli S, Rotilio G, Ciriolo MR (2008) Role of nitric oxide synthases in Parkinson's disease: a review on the antioxidant and anti-inflammatory activity of polyphenols. Neurochem Res 33: 2416–2426.
40. Tseng KY, Caballero A, Dec A, Cass DK, Simak N, et al. (2011) Inhibition of Striatal Soluble Guanylyl Cyclase-cGMP Signaling Reverses Basal Ganglia Dysfunction and Akinesia in Experimental Parkinsonism. PLoS One 6: e27187.
41. Suzuki N, Motohashi N, Uezumi A, Fukada S, Yoshimura T, et al. (2007) NO production results in suspension-induced muscle atrophy through dislocation of neuronal NOS. J Clin Invest 117: 2468–2476.
42. Soh JW, Kazi JU, Li H, Thompson WJ, Weinstein IB (2008) Celecoxib-induced growth inhibition in SW480 colon cancer cells is associated with activation of protein kinase G. Mol Carcinog 47: 519–525.
43. Kwon IK, Wang R, Thangaraju M, Shuang H, Liu K, et al. (2010) PKG inhibits TCF signaling in colon cancer cells by blocking beta-catenin expression and activating FOXO4. Oncogene 29: 3423–3434.
44. Lee KS, Iijima-Ando K, Iijima K, Lee WJ, Lee JH, et al. (2009) JNK/FOXO-mediated neuronal expression of fly homologue of peroxiredoxin II reduces oxidative stress and extends life span. J Biol Chem 284: 29454–29461.
45. Hong YK, Lee NG, Lee MJ, Park MS, Choi G, et al. (2009) dXNP/DATRX increases apoptosis via the JNK and dFOXO pathway in Drosophila neurons. Biochem Biophys Res Commun 384: 160–166.
46. Wang MC, Bohmann D, Jasper H (2005) JNK extends life span and limits growth by antagonizing cellular and organism-wide responses to insulin signaling. Cell 121: 115–125.
47. Puig O, Marr MT, Ruhf ML, Tjian R (2003) Control of cell number by Drosophila FOXO: downstream and feedback regulation of the insulin receptor pathway. Genes Dev 17: 2006–2020.
48. McGettigan J, McLennan RK, Broderick KE, Kean L, Allan AK, et al. (2005) Insect renal tubules constitute a cell-autonomous immune system that protects the organism against bacterial infection. Insect Biochem Mol Biol 35: 741–754.
49. Venderova K, Kabbach G, Abdel-Messih E, Zhang Y, Parks RJ, et al. (2009) Leucine-Rich Repeat Kinase 2 interacts with Parkin, DJ-1 and PINK-1 in a Drosophila melanogaster model of Parkinson's disease. Hum Mol Genet 18: 4390–4404.
50. Osterwalder T, Yoon KS, White BH, Keshishian H (2001) A conditional tissue-specific transgene expression system using inducible GAL4. Proc Natl Acad Sci U S A 98: 12596–12601.
51. Udan RS, Kango-Singh M, Nolo R, Tao C, Halder G (2003) Hippo promotes proliferation arrest and apoptosis in the Salvador/Warts pathway. Nat Cell Biol 5: 914–920.
52. Lu Y, Wu LP, Anderson KV (2001) The antibacterial arm of the drosophila innate immune response requires an IkappaB kinase. Genes Dev 15: 104–110.
53. Jia J, Tong C, Wang B, Luo L, Jiang J (2004) Hedgehog signalling activity of Smoothened requires phosphorylation by protein kinase A and casein kinase I. Nature 432: 1045–1050.
54. Junger MA, Rintelen F, Stocker H, Wasserman JD, Vegh M, et al. (2003) The Drosophila forkhead transcription factor FOXO mediates the reduction in cell number associated with reduced insulin signaling. J Biol 2: 20.
55. Yakubovich N, Silva EA, O'Farrell PH (2010) Nitric oxide synthase is not essential for Drosophila development. Curr Biol 20: R141–142.
56. Muller D, Kugler SJ, Preiss A, Maier D, Nagel AC (2005) Genetic modifier screens on Hairless gain-of-function phenotypes reveal genes involved in cell differentiation, cell growth and apoptosis in Drosophila melanogaster. Genetics 171: 1137–1152.
57. Yang Y, Gehrke S, Imai Y, Huang Z, Ouyang Y, et al. (2006) Mitochondrial pathology and muscle and dopaminergic neuron degeneration caused by

inactivation of Drosophila Pink1 is rescued by Parkin. Proc Natl Acad Sci U S A 103: 10793–10798.
58. Zhang X, Gan L, Pan H, Guo S, He X, et al. (2002) Phosphorylation of serine 256 suppresses transactivation by FKHR (FOXO1) by multiple mechanisms. Direct and indirect effects on nuclear/cytoplasmic shuttling and DNA binding. J Biol Chem 277: 45276–45284.
59. Yuasa K, Michibata H, Omori K, Yanaka N (2000) Identification of a conserved residue responsible for the autoinhibition of cGMP-dependent protein kinase Ialpha and beta. FEBS Lett 466: 175–178.
60. Imai Y, Soda M, Inoue H, Hattori N, Mizuno Y, et al. (2001) An unfolded putative transmembrane polypeptide, which can lead to endoplasmic reticulum stress, is a substrate of Parkin. Cell 105: 891–902.
61. Imai Y, Soda M, Takahashi R (2000) Parkin suppresses unfolded protein stress-induced cell death through its E3 ubiquitin-protein ligase activity. J Biol Chem 275: 35661–35664.
62. Kwon Y, Hofmann T, Montell C (2007) Integration of phosphoinositide- and calmodulin-mediated regulation of TRPC6. Mol Cell 25: 491–503.

Saito et al. Molecular Neurodegeneration 2012, 7:50
http://www.molecularneurodegeneration.com/content/7/1/50

MOLECULAR NEURODEGENERATION

RESEARCH ARTICLE Open Access

Hyperpolarization-activated cyclic nucleotide gated channels: a potential molecular link between epileptic seizures and Aβ generation in Alzheimer's disease

Yuhki Saito[1], Tsuyoshi Inoue[2], Gang Zhu[3], Naoki Kimura[1], Motohiro Okada[4], Masaki Nishimura[5], Nobuyuki Kimura[6], Shigeo Murayama[7,8], Sunao Kaneko[9], Ryuichi Shigemoto[10], Keiji Imoto[11] and Toshiharu Suzuki[1*]

Abstract

Background: One of the best-characterized causative factors of Alzheimer's disease (AD) is the generation of amyloid-β peptide (Aβ). AD subjects are at high risk of epileptic seizures accompanied by aberrant neuronal excitability, which in itself enhances Aβ generation. However, the molecular linkage between epileptic seizures and Aβ generation in AD remains unclear.

Results: X11 and X11-like (X11L) gene knockout mice suffered from epileptic seizures, along with a malfunction of hyperpolarization-activated cyclic nucleotide gated (HCN) channels. Genetic ablation of HCN1 in mice and HCN1 channel blockage in cultured Neuro2a (N2a) cells enhanced Aβ generation. Interestingly, HCN1 levels dramatically decreased in the temporal lobe of cynomolgus monkeys (*Macaca fascicularis*) during aging and were significantly diminished in the temporal lobe of sporadic AD patients.

Conclusion: Because HCN1 associates with amyloid-β precursor protein (APP) and X11/X11L in the brain, genetic deficiency of X11/X11L may induce aberrant HCN1 distribution along with epilepsy. Moreover, the reduction in HCN1 levels in aged primates may contribute to augmented Aβ generation. Taken together, HCN1 is proposed to play an important role in the molecular linkage between epileptic seizures and Aβ generation, and in the aggravation of sporadic AD.

Background

Alzheimer's disease (AD) is characterized by progressive memory impairment, which accompanies aging. Genetic and biochemical studies show that the production of amyloid-β peptide (Aβ) largely contributes to the etiology of AD [1]. Aβ is generated from amyloid-β precursor protein (APP) by β- and γ-cleavage of the latter.

The risk of seizure activity is particularly high in AD patients, with an 87-fold increase in subjects with early-onset dementia compared with an age-matched reference population [2-7]. Factors linking seizure activity to Aβ generation in AD patients remain unclear, although epilepsy is believed to result from abnormal regulation of neuronal excitability, which favors hypersynchrony. In addition, increased neuronal activity enhances Aβ production from APP [8-10].

Hyperpolarization-activated cyclic nucleotide gated HCN channels 1–4 (HCN1–4) conduct inward, depolarizing mixed Na^+/K^+ currents and thereby control resting membrane potential, dendritic integration, synaptic transmission, and rhythmic activity in cardiac pacemaker cells and spontaneous firing neurons [11]. Dysregulation of these channels and their hyperpolarization-activated (Ih) currents is strongly implicated in various experimental animal models of epilepsy, as well as in human epilepsy patients [12]. Furthermore, HCN2 co-assembles with the X11-like (X11L) protein [13], which is a metabolic regulator of APP processing [14].

X11 proteins (X11s) comprise a family of three evolutionarily conserved molecules (X11/X11α/Mint1, X11L/

* Correspondence: tsuzuki@pharm.hokudai.ac.jp
[1]Laboratory of Neuroscience, Graduate School of Pharmaceutical Sciences, Hokkaido University, Kita12-Nishi6, Kita-ku, Sapporo 060-0812, Japan
Full list of author information is available at the end of the article

X11β/Mint2, and X11L2/X11γ/Mint3). These proteins bind to the cytoplasmic region of APP in cultured cells and suppress its metabolism [15,16]. Moreover, the metabolism of overexpressed human APP (hAPP) is suppressed in X11 and X11L transgenic mice, along with the generation of Aβ [17-19]. On the other hand, mutant mice lacking X11L ($X11^{+/+}/X11L^{-/-}$ mice) or both X11 and X11L ($X11^{-/-}/X11L^{-/-}$ mice) facilitate amyloidogenic metabolism of endogenous murine APP and exogenous hAPP, including Aβ generation [20-22]. Therefore, inactivation of X11/X11L clearly increases the production of Aβ, potentially contributing to the pathology of AD.

Here, we report that i) $X11^{-/-}/X11L^{-/-}$ mice suffer from spontaneous epileptic seizures along with malfunction of HCN channel activity; ii) HCN1 can form a complex with APP and X11 or X11L in the murine brain; iii) $HCN1^{-/-}$ gene knockout mice show enhanced Aβ generation; iv) overexpression of HCN1 in Neuro2a (N2a) cells decreases Aβ generation, whereas blockage of HCN1 channel activity in N2a cells restores the level of Aβ production; v) the level of HCN1 diminishes significantly in the temporal cortex of cynomolgus monkeys (*Macaca fascicularis*) during aging; and vi) HCN1 levels are significantly reduced in the brains of sporadic AD patients compared with the brains of age-matched healthy subjects.

Given the previous reports and our current observations, we hypothesize that X11 and X11L play an important role in the modulation of HCN channel function, the dysregulation of which correlates with epilepsy. We further hypothesize that the impairment of HCN channels, and in particular HCN1, accompanies with the aberrant production of Aβ, which manifests as neurotoxicity. Thus, HCN1 together with X11 and X11L may provide a molecular link between seizure activity and Aβ generation in AD patients.

Results

Spontaneous epileptic seizures caused by X11 and X11L gene deficiency

Electrocorticograms were recorded in $X11^{+/+}/X11L^{+/+}$ (wild type), $X11^{+/+}/X11L^{-/-}$, $X11^{-/-}/X11L^{+/+}$, and $X11^{-/-}/X11L^{-/-}$ mice. We found that $X11^{-/-}/X11L^{-/-}$ mice suffered from spontaneous epileptic seizures at the age of 13 weeks and over (detailed results are provided in Additional file 1: Figure S1 and Additional file 2: Movies S1, Additional file 3: Movies S2 and Additional file 4: Movies S3). Three out of four $X11^{-/-}/X11L^{-/-}$ mice showed an abnormal electrocorticogram recording within 48 h, namely, the presence of epileptic discharge, which were never observed in $X11^{+/+}/X11L^{+/+}$, $X11^{+/+}/X11L^{-/-}$, or $X11^{-/-}/X11L^{+/+}$

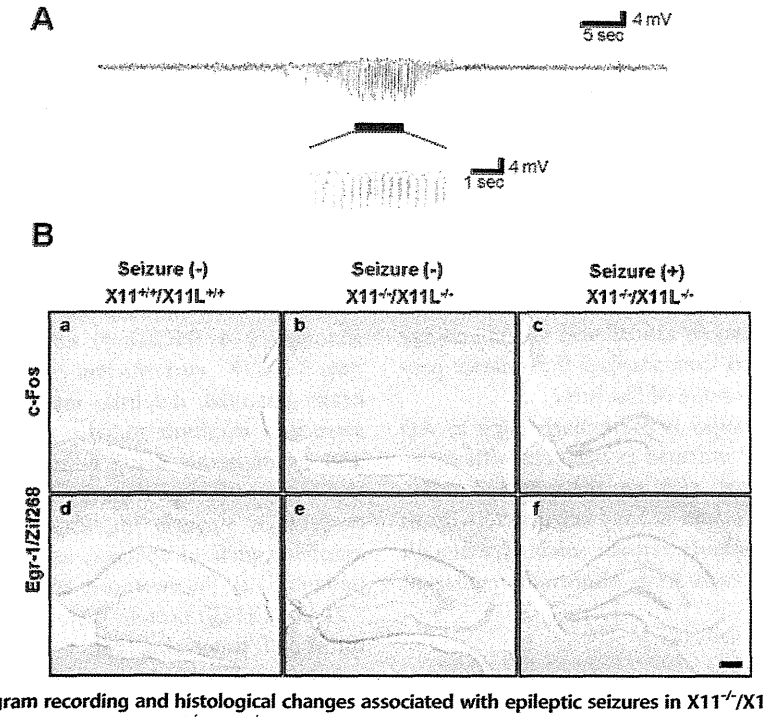

Figure 1 Electrocorticogram recording and histological changes associated with epileptic seizures in $X11^{-/-}/X11L^{-/-}$ mice. (*A*) An electrocorticogram recorded in 13-week-old $X11^{-/-}/X11L^{-/-}$ mice (n = 4). Epileptic discharges are underlined. (*B*) c-Fos (*a, b, c*) and Egr-1/zif268 (*d, e, f*) immunoreactivity in the hippocampus of $X11^{+/+}/X11L^{+/+}$ (*a, d*) and $X11^{-/-}/X11L^{-/-}$ (*b, c, e, f*) mice under steady-state conditions (*a, b, d, e*) and at 90 min after an epileptic episode (*c, f*). Scale bar, 200 μm.

mice (Figure 1, Additional file 1: Figure S1 and Additional file 4: Movie S3). Subsets of $X11^{-/-}/X11L^{-/-}$ mice went into status epilepticus and died.

Seizures are often associated with the augmented expression of immediate-early genes in neurons [23]. We first asked whether such gene activation was observed in $X11^{-/-}/X11L^{-/-}$ mice following epileptic seizures and investigated the involvement of specific brain regions in seizure activity. Brain tissue sections from $X11^{-/-}/X11L^{-/-}$ mice were immunostained for c-Fos, a calcium-dependent immediate-early gene product, and Egr-1/Zif268, an early growth response transcription factor, within 90 min of a seizure event. The brains of these mice showed enhanced expression of both c-Fos and Egr-1/Zif268 in the dentate gyrus (DG) granule cells compared with the brains of $X11^{+/+}/X11L^{+/+}$ and $X11^{-/-}/X11L^{-/-}$ mice (Figure 1B). However, we cannot rule out a possibility that subclinical discharges without aberrant behavior may

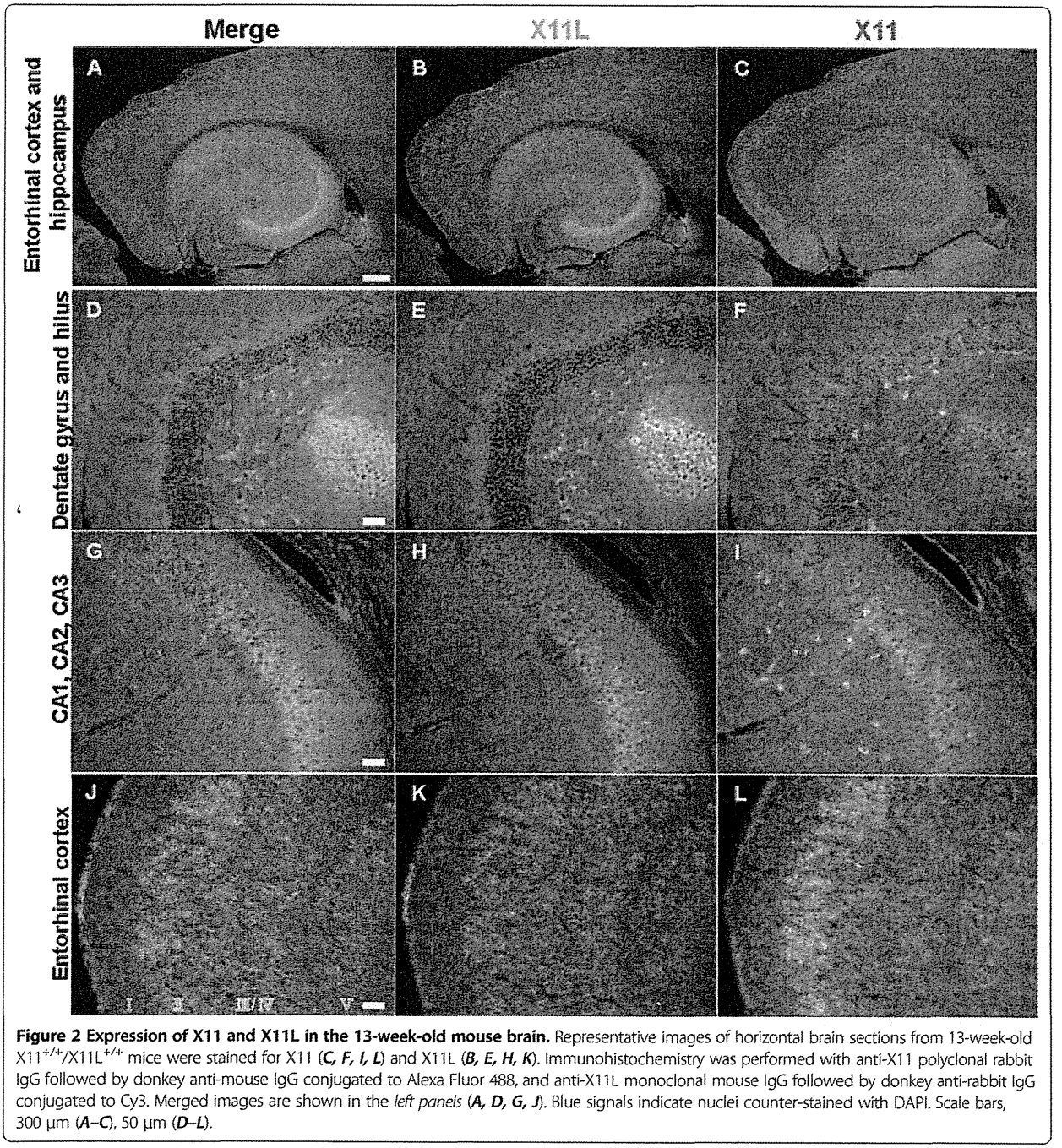

Figure 2 Expression of X11 and X11L in the 13-week-old mouse brain. Representative images of horizontal brain sections from 13-week-old $X11^{+/+}/X11L^{+/+}$ mice were stained for X11 (***C, F, I, L***) and X11L (***B, E, H, K***). Immunohistochemistry was performed with anti-X11 polyclonal rabbit IgG followed by donkey anti-mouse IgG conjugated to Alexa Fluor 488, and anti-X11L monoclonal mouse IgG followed by donkey anti-rabbit IgG conjugated to Cy3. Merged images are shown in the *left panels* (***A, D, G, J***). Blue signals indicate nuclei counter-stained with DAPI. Scale bars, 300 μm (***A–C***), 50 μm (***D–L***).

cause the enhanced expression of c-Fos and Egr-1/Zif268. Thus, a deficiency in both X11 and X11L may cause abnormal, seizure-associated neuronal activity and subsequent alterations in protein expression in the hippocampal formation.

Reduction of Ih currents in entorhinal cortex (EC) layer II of $X11^{-/-}/X11L^{-/-}$ mice

Spontaneous epileptic seizures were observed in mice when both X11 and X11L genes were deficient (Figure 1A, Additional file 1: Figure S1 and additional movies). Because the DG granule cells of $X11^{-/-}/X11L^{-/-}$ mice showed augmented expression of c-Fos and Egr-1/Zif268 following seizure activity, we next performed a detailed examination of the expression of both proteins in hippocampal neurons in 13-week-old murine brains (Figure 2).

Distinct expression patterns of X11 and X11L were observed in the hippocampus of wild type mice. X11L was expressed mainly in the pyramidal neurons of the CA1–3 region (Figure 2B, E, H), whereas X11 was expressed in other types of interneurons (Figure 2C, F, I). These observations coincide with our previous report of X11s expression in aged wild type mice [21]. Unlike c-Fos and Egr-1/Zif268 in the double mutant mouse, X11 and X11L were not expressed in DG granule cells (Figure 2D–F). However, both X11 and X11L were strongly co-expressed in EC layer II (Figure 2J–L), which projects axons primarily to the granule cells of the DG [24]. Furthermore, both HCN1 and HCN2 are expressed in EC layer II [25]. Given that $HCN1^{-/-}$ mice show enhanced seizure susceptibility and that $HCN2^{-/-}$ mice suffer from absence seizures [26,27], we next focused our investigations on the alteration of Ih currents associated with HCN channels in EC layer II in $X11^{-/-}/X11L^{-/-}$ mice.

Horizontal brain slices that included the EC and the hippocampus were prepared from 12–14-week-old $X11^{+/+}/X11L^{+/+}$, $X11^{+/+}/X11L^{-/-}$, $X11^{-/-}/X11L^{+/+}$, and $X11^{-/-}/X11L^{-/-}$ mice. EC layer II neurons were then subjected to electrophysiological analysis, and Ih currents from HCN channels were recorded (Figure 3 and Additional file 1: Figure S2). The mice used in the electrophysiological study were seizure-naïve, at least without over behavioral manifestations, and showed comparable levels of HCN1 channels in the EC (Additional file 1: Figure S3). Similar to a previous report [28], hyperpolarizing voltage steps activated a large Ih current in EC layer II cells of $X11^{+/+}/X11L^{+/+}$ mice (Figure 3A and C). By contrast, the Ih current was dramatically reduced in $X11^{-/-}/X11L^{-/-}$ mice relative to that in $X11^{+/+}/X11L^{+/+}$ mice (Figure 3B and D); however, no significant alterations were observed for the V1/2 (mean ± SEM, $X11^{+/+}/X11L^{+/+}$: −81.1±1.1 mV; $X11^{-/-}/X11L^{+/+}$: −80.3±1.3 mV; $X11^{+/+}/X11L^{-/-}$: −83.5±1.4 mV; $X11^{-/-}/X11L^{-/-}$: −81.3±0.9 mV) (Figure 3E) or the series resistance (mean ± SEM, $X11^{+/+}/X11L^{+/+}$: 8.3±0.2 MΩ; $X11^{-/-}/X11L^{+/+}$: 8.9±0.5 MΩ; $X11^{+/+}/X11L^{-/-}$: 9.2±0.4 MΩ; $X11^{-/-}/X11L^{-/-}$: 8.0±0.2 MΩ) (Figure 3F). Quantitative analysis (Figure 3G) revealed that the density of the Ih current was also significantly reduced in $X11^{-/-}/X11L^{-/-}$ mice (1.12±0.15 pA/pF, n = 9; $p < 0.01$) compared with that in $X11^{+/+}/X11L^{+/+}$ mice (2.18±0.27 pA/pF, n = 10), but did not change significantly in $X11^{-/-}/X11L^{+/+}$ mice (2.41±0.25 pA/pF, n = 9, $p > 0.05$) or in $X11^{+/+}/X11L^{-/-}$ mice (2.05±0.29 pA/pF, n = 9, $p > 0.05$). Thus, genetic ablation of X11 and X11L together had a profound impact on the Ih current in the EC layer II of the double knockout mice. These results correlate with the observation that $X11^{-/-}/X11L^{-/-}$ mice, but not $X11^{+/+}/X11L^{+/+}$, $X11^{+/+}/X11L^{-/-}$, or $X11^{-/-}/X11L^{+/+}$ mice, are susceptible to spontaneous epileptic seizures.

In EC layer II, the dominant HCN subtype is HCN1 [28]. We found that HCN1, X11, and X11L were colocalized in EC layer II neurons (Figure 3H) and apparently formed a complex in the brain (Figure 3I–K). The colocalization of these molecules was observed in a region surrounding the neuronal nucleus (Figure 3H), consistent with the location of the Golgi apparatus. Because X11 and X11L are largely localized in the Golgi apparatus and function in the trafficking of membrane proteins [29,30], the deletion of X11 and X11L may disturb intracellular localization of HCN channels (Additional file 1: Figure S4). While the localization of the channel likely affects its function, we cannot rule out the possibility that X11 and X11L directly regulate HCN1 function as well.

Enhanced Aβ generation according to HCN1 dysfunction

The EC is one of the most vulnerable brain regions in AD [31], and it is well-known that synaptic activity such as that mediated by HCN channels can regulate Aβ generation [8-10]. Therefore, we examined whether HCN channel impairment involved in the aberrant production of Aβ. We first quantified the levels of endogenous Aβ40 and Aβ42 in $HCN1^{-/-}$ mouse brains. Aβ40 and Aβ42 were both significantly increased in the cortex of $HCN1^{-/-}$ mice compared with $HCN1^{+/+}$ mice (average ± SEM, Aβ40: n = 5, $p = 0.0037$; Aβ42: n = 5, $p = 0.0055$) (Figure 4A). The magnitude of the increase in Aβ40 and Aβ42 was inversely proportional to the level of HCN1 gene expression (Figure 4A, left panel), while APP protein levels were comparable in $HCN1^{+/+}$, $HCN1^{+/-}$, and $HCN1^{-/-}$ mice (Figure 4A, right panel).

To confirm whether the increase in Aβ generation in $HCN1^{-/-}$ mice depends on the decrease in HCN channel activity, we used N2a cells that transiently overexpressed FLAG-APP and HCN1 (Figure 4B). Overexpression of HCN1 significantly reduced the generation of Aβ40 and Aβ42 (compare column 2 with column 3 for each Aβ peptide). The Aβ levels were restored by adding ZD7288, a

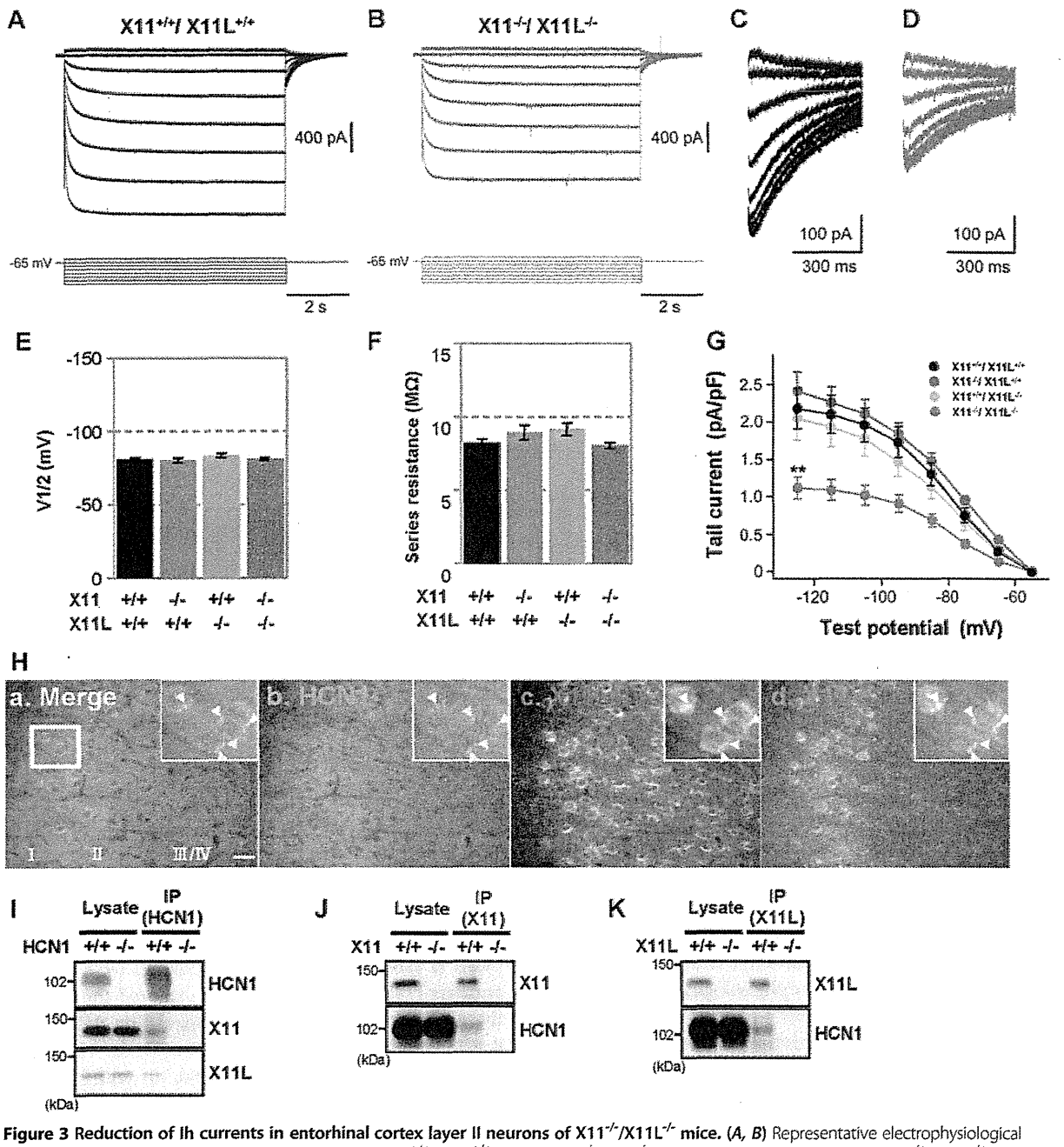

Figure 3 Reduction of Ih currents in entorhinal cortex layer II neurons of $X11^{-/-}/X11L^{-/-}$ mice. (*A, B*) Representative electrophysiological recordings of Ih currents from EC layer II neurons in $X11^{+/+}/X11L^{+/+}$ (*A*) and $X11^{-/-}/X11L^{-/-}$ (*B*) mice. (*C, D*) Tail currents of $X11^{+/+}/X11L^{+/+}$ (*C*) and $X11^{-/-}/X11L^{-/-}$ (*D*) mice. (*E*) Quantitative data of the voltage, whereby the current is half-activated (V1/2). Statistical analysis was performed using one-way analysis of variance followed by Tukey's multiple comparison test (mean ± SEM (mV); five slices from two $X11^{+/+}/X11L^{+/+}$ mice, n = 10; four slices from two $X11^{-/-}/X11L^{+/+}$, $X11^{+/+}/X11L^{-/-}$, and $X11^{-/-}/X11L^{-/-}$ mice, n = 9). (*F*) Quantitative data of series resistance. Statistical analysis was performed as described (mean ± SEM (MΩ); five slices from two $X11^{+/+}/X11L^{+/+}$ mice, n = 10; four slices from two $X11^{-/-}/X11L^{+/+}$, $X11^{+/+}/X11L^{-/-}$, and $X11^{-/-}/X11L^{-/-}$ mice, n = 9). (*G*) Summary of the current density of the tail currents. Statistical analysis was performed as described (mean ± SEM (pA/pF); five slices from two $X11^{+/+}/X11L^{+/+}$ mice, n = 10; four slices from two $X11^{-/-}/X11L^{+/+}$, $X11^{+/+}/X11L^{-/-}$, and $X11^{-/-}/X11L^{-/-}$ mice, n = 9; $^{**}p < 0.01$). (*H*) Representative images of the HCN1-X11-X11L complex in EC layer II neurons of 13-week-old $X11^{+/+}/X11L^{+/+}$ mice (a, merge; b HCN1 (green); c, X11L (red); d, X11(blue)). Scale bar, 20 μm. (*I–K*) Co-immunoprecipitation of HCN1-X11s complexes from the 13-week-old $X11^{+/+}/X11L^{+/+}$ murine cortex. $HCN1^{-/-}$ (*I*), $X11^{-/-}$ (*J*), or $X11L^{-/-}$ (*K*) mice were used as controls. Brain lysates were immunoprecipitated with anti-HCN1 (*I*), anti-X11 (*J*), and anti-X11L/Mint2 (*K*) antibodies. Immunocomplexes were detected by immunoblotting.